ARTICLE

Reactivities of Electrophilic N−F Fluorinating Reagents

Neshat Rozatian[a], David R. W. Hodgson*[a]

Electrophilic fluorination represents one of the most direct and useful methods available for the selective introduction of fluorine into organic compounds. Electrophilic fluorinating reagents of the N−F class have revolutionised the incorporation of fluorine atoms into both pharmaceutically- and agrochemically-important substrates. Since the earliest N−F reagents were commercialised in the 1990s, their reactivities have been investigated using qualitative and, more recently, quantitative methods. This review discusses the different experimental approaches employed to determine reactivities of N−F reagents, focussing on the kinetics studies reported in recent years. We make critical evaluations of the experimental approaches against each other, theoretical approaches, and their applicability towards practical problems. The opportunities for achieving more efficient synthetic electrophilic fluorination processes through kinetic understanding are highlighted.

1. Introduction

Organofluorine compounds form an important family of molecules that have significant roles in medicinal, agrochemical and material sciences due to the unique properties of the fluorine atom.[1–4] Several properties of organic compounds can be altered by incorporation of a fluorine atom, including pK_a, lipophilicity, protein binding affinity and metabolic stability.[1] Consequently, pharmaceuticals bearing fluoro-aliphatic, -aromatic and -heterocyclic units have been developed, such as Prozac™, Lipitor®, Emtriva®, Flonase®, Sovaldi®, Januvia® and Crestor®.[5,6] Indeed, 30% of pharmaceuticals introduced to the market in 2018 contained fluorine,[7] and around 50% of the most successful "blockbuster" drugs are fluorine-containing compounds.[8] In 1954, Fried and Sabo discovered that the introduction of a single fluorine atom into the corticosteroid **4** (fludrocortisone) increased its potency tenfold (**Figure 1**).[9] 5-Fluorouracil **5** was developed as an anti-cancer drug,[10] and its analogue, 5-fluorocytosine, was introduced as an anti-fungal agent. The development of 6-fluoroquinolones in the 1980s led to a large class of bactericides, where ciprofloxacin **6** is one of the most widely used antibiotics worldwide. The discovery of pharmaceuticals bearing −CF₂, −CF₃ and −CF₂CF₃ moieties has led to a diversification in the field in more recent years. Pantoprazole **7**, containing the CF₂ moiety, is used to treat stomach ulcers and esophagitis, and in 2017 was the 19th most prescribed medication in the United States.[11]

Fluorine is the most abundant halogen; it is present in various ores in the earth's crust. The main mineral sources of fluorine are fluorspar (CaF_2), cryolite (Na_3AlF_6) and fluorapatite ($Ca_5(PO_4)_3F$).[12,13] However, organofluorine compounds are very scarce in nature.[14] Currently, all fluorine atoms used for organofluorine chemistry originate from fluorspar, which is

converted to anhydrous hydrogen fluoride (aHF) using aqueous sulfuric acid. aHF is directly employed in many industrial processes, including Balz-Schiemann and Swarts halogen exchange processes for the manufacture of fluoroaromatic and trifluoromethylaromatic derivatives, respectively.[12] aHF is used for the preparation of the next generation of fluorinating reagents, including F₂, KF and Et₃N.3HF. These are reacted further with the appropriate substrates to obtain the fluorinating reagents that are most commonly used in laboratory-scale discovery processes. These reagents are often separated into two main classes: nucleophilic and electrophilic agents. Several commercially available, shelf-stable reagents of both classes have been developed, thus avoiding the need for specialist equipment or lengthy preparations. Nucleophilic fluorinating reagents include DAST and Deoxo-Fluor™, which are employed for the conversion of C−O bonds to C−F bonds. For the conversion of electron-rich centres, such as the direct conversion of C−H to C−F linkages, nucleophilic fluorinating agents are usually not feasible. In these cases, electrophilic sources of fluorine are employed, such as Selectfluor™ and NFSI.

Early investigations into the development of electrophilic fluorinating reagents centred on those bearing an O−F bond (e.g. CF₃OF,[15,16] ClO₃F,[17,18] CF₃COOF,[19] CH₃COOF,[20] CsSO₄F[21]), or an Xe−F bond (i.e. XeF₂).[22,23] However, these reagents were often too reactive, unselective, difficult to prepare and not available commercially. Elemental fluorine (F₂) has been successfully used for the fluorination of a range of nucleophilic substrates using both batch and flow techniques.[24–30] However, the safe use of F₂ on both laboratory and manufacturing scales requires specialist handling techniques and equipment that are not widely available.

The introduction of bench-stable electrophilic fluorinating reagents containing an N−F bond in the 1980s revolutionised this field.[31] The N−F reagents are selective and easy-to-handle sources of electrophilic fluorine, many of which are now commercially available and do not require specialized handling

procedures. N−F reagents can be divided into two classes: (i) neutral N−F reagents and (ii) quaternary ammonium N−F reagents, of which the quaternary salts are considered to be the most electrophilic. The popularity and broad synthetic application of N−F reagents are partly due to their long shelf lives, and the fact that they can be handled safely in glassware.
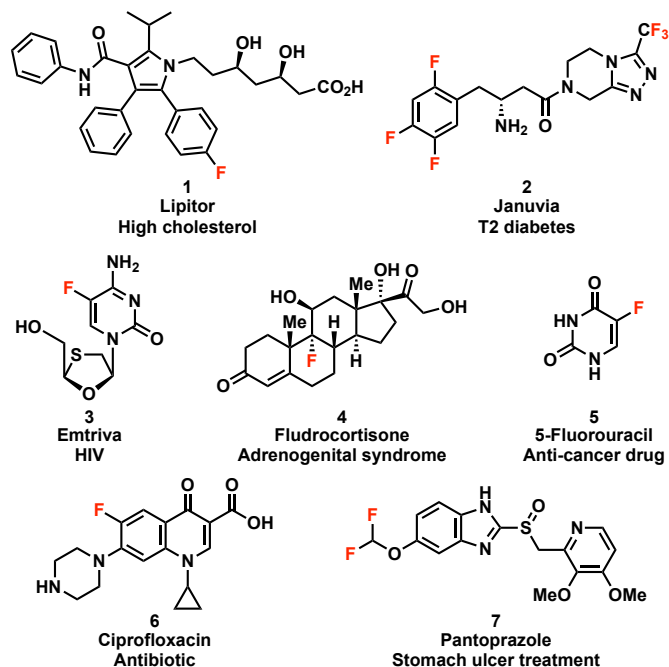

Figure 1: Examples of fluorine-containing drugs.

Examples of N−F reagents reported from 1964-2018 are presented in **Figure 2**. The main commercial reagents of this class include *N*-fluoropyridinium salts (such as salts **14**-**19**) developed by Umemoto *et al.*,[32–34] NFSI (*N*-fluorobenzenesulfonimide, **23**) developed by Differding,[35] and Selectfluor™ (1-chloromethyl-4-fluoro-1,4-diazoniabicyclo[2.2.2]octane bis[tetrafluoroborate], **25**) developed by Banks *et al*.[36] Stavber and co-workers developed an analogue of Selectfluor™, which was named Accufluor™ (1-fluoro-4-hydroxy-1,4-diazoniabicyclo[2.2.2]octane bis[tetrafluoroborate], **27**).[37] The current widespread interest in the development of novel fluorinating reagents is demonstrated by the fact that several groups, including those of Shibata, Toste and Gouverneur, have reported new reagents in recent years. These contributions include a sterically demanding version of NFSI described by Shibata, *N*-fluoro-(3,5-di-*tert*-butyl-4-methoxy)benzenesulfonimide (NFBSI, **36**)[38] and chiral analogues (**38**).[39] Gouverneur *et al*. reported chiral Selectfluor™ derivatives in 2013 (**39**),[40] followed by a novel N−F reagent derived from the ethano-Tröger's base in 2016 (**40**).[41] Most recently, in 2018, a new generation of radical N−F fluorinating reagents based on *N*-fluoro-*N*-arylsulfonamides **41** were reported by Zipse and Renaud.[42]

Since its discovery, Selectfluor™ **25** has rapidly become a commercial chemical produced on a multi-ton scale, and is now one of the most popular N−F reagents.[43] Every year, 25 tonnes of Selectfluor™ **25** sell for $7.5 million.[44] This reagent is widely used for both small-scale laboratory applications and moderate-scale industrial syntheses, and it also plays an important role in medicinal and drug discovery applications. Selectfluor™ **25** is thermally stable up to 195 °C,[43] has moderate to high solubility and stability in polar solvents (water, MeCN, DMF, methanol, THF) and has low toxicity. 80% of all commercially available fluorosteroids are synthesised industrially using Selectfluor™ **25**,[44] which replaced highly corrosive reagents such as perchloryl fluoride (ClO$_3$F).[5,45] Indeed, fluticasone propionate **44** (**Scheme 1a**) is one of the most prescribed pharmaceutical fluorosteroid products. Between 2009 and 2012, global sales of fluticasone propionate-containing therapeutics totalled approximately $17 billion.[44]

N−F reagents have been employed for the fluorination of several drug targets.[46] A team at Merck fluorinated the sodium salt of malonate **45** using Selectfluor™ **25** in THF, towards the synthesis of cMET tyrosine kinase inhibitors for anti-cancer applications (**Scheme 1b**).[47] In 2014, Gilead Sciences reported the successful use of NFSI **23** to achieve the difluorination of fluorene to synthesise ledipasvir **50**, a therapeutic for the treatment of hepatitis C (**Scheme 1c**).[48] A kilogram-scale enantioselective fluorination using NFSI **23** was reported in 2015 by GlaxoSmithKline for the synthesis of a tyrosine kinase (Syk) inhibitor as a preclinical drug candidate (**Scheme 1d**).[49] NFSI **23** was used in the asymmetric fluorination of prochiral malonate esters, which were further employed as building blocks for the preparation of pharmaceutically-relevant compounds, including fluorinated β-amino acids, β-lactams and protease inhibitors (**Scheme 1e**).[50] A method for the preparation of the fluorine-containing antibiotic solithromycin was carried out by reacting **57** with NFSI **23** to obtain solithromycin precursor **58** (**Scheme 1f**).[51]

Due to the high reactivities of many early fluorinating reagents (CF$_3$OF, CsSO$_4$F, XeF$_2$) as well as their high sensitivities to reaction conditions, quantitative analyses of reactions involving these electrophilic fluorinating agents are scarce. Three examples of kinetics studies have been reported: by Appelman and co-workers[52] in 1981 (reactions of fluoroxysulfate with aromatic compounds), oxytrifluoromethylation kinetics studied by Levy and Sterling[53] in 1985 (reactions of CF$_3$OF with ring-substituted styrenes) and fluorination of alkenes via CsSO$_4$F and XeF$_2$ by Stavber *et al.* in 1993.[54]

The N−F reagents overcame problems associated with previous types of fluorinating agents due to their improved selectivities, stabilities and optimal reactivities. These properties made them more amenable to reactivity studies and several attempts towards ranking their reactivities have been made over the past 30 years, each employing different qualitative and quantitative experimental approaches. Very recently, several efforts towards ordering the relative reactivities of fluorination, trifluoromethylation and trifluoromethylthiolation reagents were reviewed by Cheng *et al*.[55] with a focus on the computational results of the same group. Here, we review experimental approaches towards the measurement of the reactivities of N−F reagents.

Quantification of the fluorinating powers of electrophilic N−F reagents is vital for the rational design and optimization of novel fluorinating reagents and the development of new synthetic reactions. The purpose of our review is to give a chronological discussion of all experimental and kinetics reports towards the quantification of reactivities of N−F reagents. We anticipate that this will provide a valuable resource for chemists carrying out electrophilic fluorination chemistry, will aid the pairing of fluorinating reagents with specific substrates, and may point towards opportunities for the development of novel reagents.
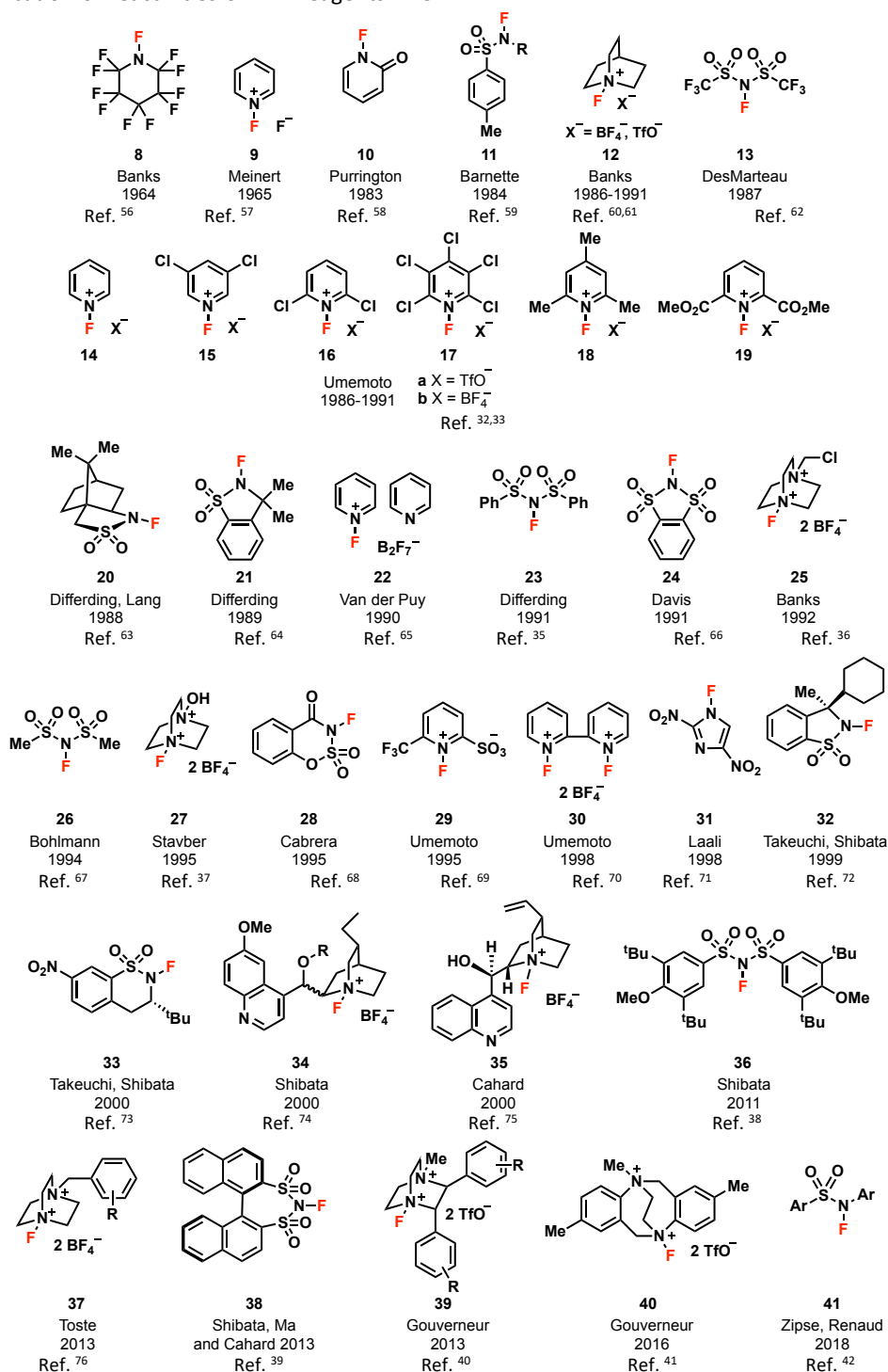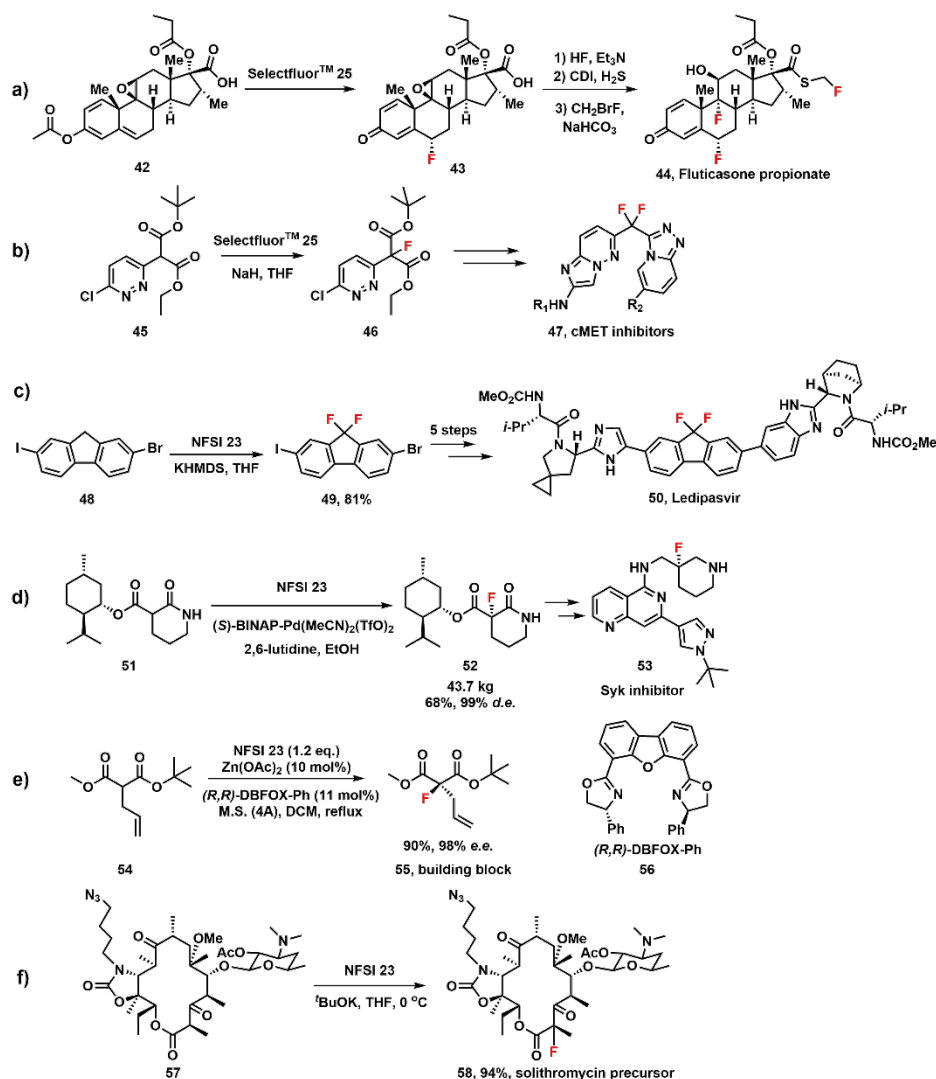

Figure 2: Examples of fluorinating reagents of the N−F class.

Scheme 1: Syntheses of fluorine-containing, pharmaceutically relevant targets using Selectfluor™ **25** and NFSI **23**.

2. Power variable scale

In 1990, Umemoto and co-workers initiated comparative reaction yield studies with their power-variable scale for *N*-fluoropyridinium salts, which centred on the electron-donating or electron-withdrawing natures of substituents on the pyridinium rings.[77] The fluorinations of different classes of nucleophiles, including aromatics, carbanions, alkyl enol ethers, vinyl esters, silyl enol ethers, enamines and alkenes were carried out with each *N*-fluoropyridinium salt, and the conversion levels were compared. The results of fluorination of anisole to give *ortho*- and *para*-fluorinated anisoles are summarised in **Table 1**. Reagents with more electron-withdrawing substituents required less harsh conditions to achieve high conversions. The limitation of this approach is that it reflected reaction yields rather than kinetics parameters, where different temperatures, reaction times and solvents were used for each experiment; hence, reactivities are only comparable in a qualitative manner.

Umemoto *et al.* also attempted to correlate the fluorinating power of *N*-fluoropyridinium salts with their ^{19}F NMR chemical shifts.[78] The aqueous pK_{aH} values of the corresponding pyridines were used as an estimate of electron density of the N−F bond. For the 4-substituted and 3,5-substituted salts, the ^{19}F NMR resonances shifted downfield with substitution by increasingly electron-withdrawing groups, hence, some correlation was observed between chemical shift and pK_{aH}. For 2,6-substituted salts, however, no clear trends were observed. Furthermore, there was no dependence of chemical shift upon the counterions.

Table 1: Fluorination of anisole using *N*-fluoropyridinium triflates.[77]

Fluorinating power	NFPy (1 equiv)	Solvent	Temp / °C	Time / h	Conversion[a] / %	Product yield[b] / %	
						o-fluoro-anisole	*p*-fluoro-anisole
	triMe-NFPy **18a**	(CHCl$_2$)$_2$	147	10	68	42	[c]
	NFPy **14a**	(CHCl$_2$)$_2$	120	18	72	36	[c]
	3,5-diCl-NFPy **15a**	(CHCl$_2$)$_2$	83	18	65	48	50
	2,6-diCO$_2$Me-NFPy **19a**	DCM	40	23	71	44	48
	2,6-diCl-NFPy **16a**	DCM	40	7	71	41	41
	pentaCl-NFPy **17a**	DCM	RT	0.25	91	36	38

[a] Determined by GC-MS. [b] Determined by GC-MS based on consumed anisole. [c] Yield not determined.

3. Reduction potentials approach

In 1992, Gilicinski *et al.* reported electrochemical measurements on ten N−F reagents.[79] Cyclic voltammetry (CV) studies were conducted to determine the peak potential of the first one-electron reduction (E_p^{red}) of the N−F reagents in MeCN or DMF at a Pt electrode. The more negative E_p^{red} values correspond to decreasing oxidising power (**Figure 3a**). The authors found a correlation between the E_p^{red} values in MeCN and reported synthetic fluorinations of aromatics through conversions and reaction times, hence proposing that the most oxidising reagent (most positive E_p^{red} value) had the greatest fluorinating power. In DMF, the same relative ordering of E_p^{red} values, and thus oxidising power, was also observed, although the absolute values were slightly different. MeCN is a very common solvent in synthetic fluorination processes, while DMF is less frequently employed.[80] One of the earliest attempts to qualitatively rank the reactivities of analogues of Selectfluor™ **25** found that the addition of an electron withdrawing group at the 4-position increased the reactivities, with the following order: CF$_3$CH$_2$ > CH$_2$Cl > Me ∼ Et ∼ C$_8$H$_{17}$, determined based on reaction yields and timescales with anisole in MeCN by Banks *et al.*[36,81] It was also observed that *N*-fluoroquinuclidinium salts **12** were noticeably less reactive than analogues of Selectfluor™ **25** towards several substrates.[36] The reduction potentials determined by Gilicinski *et al.* for Selectfluor™ **25**, the *N*-methyl analogue **25a** and *N*-fluoroquinuclidinium triflate **12** (−0.04 V, −0.09 V and −0.37 V, respectively) agree with the qualitative results.

In 1992, Differding *et al.* reported peak reduction potentials of nine N−F reagents in MeCN (**Figure 3b**).[82] The electrochemical approach was continued in 1999 by Evans *et al.*[83], who reported E_p^{red} values for six N−F reagents with tetrafluoroborate counterions (**Figure 3c**). The overall mechanism for reduction on platinum electrodes was reportedly a one-electron process, with HF as a probable product of the reduction. In 2013, Yang *et al.*[84] reported E_p^{red} values for six *para*-substituted NFSI analogues (**Figure 3d**). E_p^{red} values in the latter two studies are converted to potentials vs.

SCE (using methods described in ref. [85]) in **Figure 3** to enable comparisons. E_p^{red} values in good agreement were obtained for triMe-NFPy **18a/b** and NFPy **14a/b** in each study. E_p^{red} values for Selectfluor™ **25** in MeCN were more varied: −0.04, +0.004 and +0.17 V in each report. For NFSI **23**, highly varied E_p^{red} values were reported: −0.78, −0.54, −1.141 and −1.13 V. These incongruent values are most likely due to the different experimental conditions utilised in each report. Indeed, Gilicinski reported that the absolute values varied with gold, glassy carbon or platinum electrodes.[79]

There are other limitations associated with the reduction potentials approach. Firstly, a fundamental quantity that could provide an indication of the reactivities of N−F reagents is their electrochemical standard potential, E^o, but the reduction of N−F compounds is, in most cases, irreversible. Hence, only the E_p^{red} data are available, which are often obscured by experimental problems leading to uncertainties in the measurements and the interpretation of data. Only one study has determined the standard potential for the reduction of an N−F reagent, that of *N*-fluorosultam **21**.[86] The standard potential, E^o, was found to be −0.12 V. Furthermore, the reported reproducibility of E_p^{red} values obtained by Lal *et al.* was ± 0.05 V,[79] which limits the extent to which reagents of similar E_p^{red} can be differentiated. For example, considering the errors associated with the E_p^{red} values for triMe-NFPy TfO⁻ **18a** and NFSI **23**, the two E_p^{red} values overlap. In Section 7, comparisons will be made between the electrochemical data discussed here and the rate constants from kinetics studies discussed in Section 6. In general, however, the use of *thermodynamic* parameters, such as E_p^{red} values, as gauges of the *kinetic* property of 'reactivity', must be cautioned. There are, however, many examples of thermodynamic parameters, such as pK_a values, being productively correlated with observed bimolecular rate constants to form linear free energy relationships, such as those seen in Hammett and BrØnsted relationships. In these cases, 'good' correlation only tends to occur across homologous series of similarly structured substrates. In the case of the N−F reagents, this possibility is somewhat limited by the diverse array of structures presented across the commonly employed reagent spectrum.

4. Computational investigations

One of the earliest attempts towards quantitatively ranking the reactivities of the electrophilic fluorinating reagents was a report by Christe and Dixon in 1992.[87] Based on local density functional (LDF) calculations, a scale of F⁺ detachment (FPD) energies was developed for a series of so-called oxidative
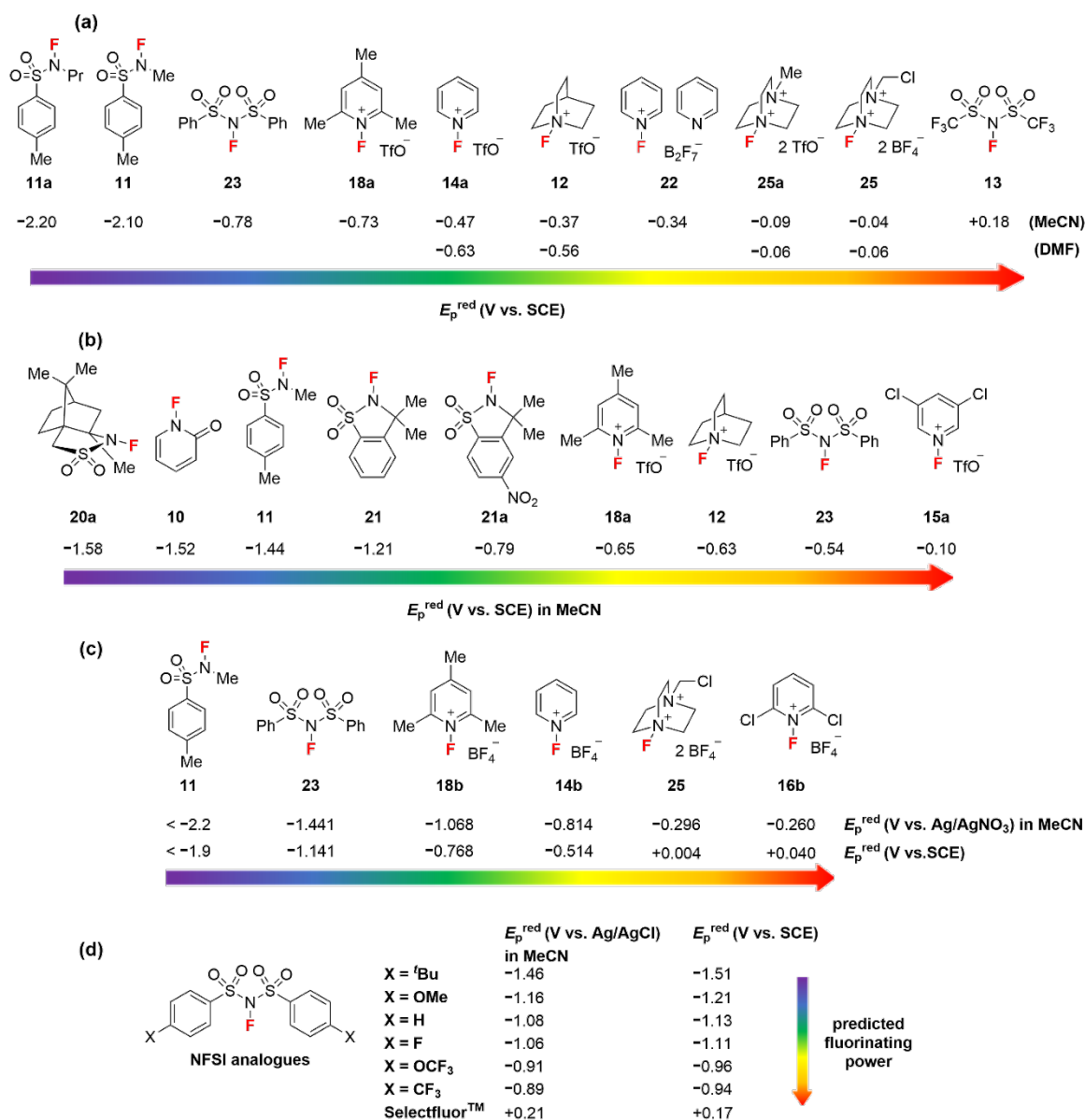
Figure 3: (a) Peak reduction potentials, E_p^{red}, in MeCN and DMF for ten N−F reagents determined by Gilicinski et al.[79] (b) Peak reduction potentials for nine N−F reagents determined by Differding et al.[82] (c) Cathodic peak potentials for six N−F reagents in MeCN determined by Evans et al.[83] and values converted to potential vs. SCE using ref.[85] (0.3 V added to values). (d) Peak reduction potentials in MeCN obtained by Yang et al.[84] and values converted to potential vs. SCE using ref.[85] (0.045 V subtracted from values).

fluorinators with the general formula XF_n^+. These values were (in kJ mol⁻¹): KrF^+ (484.9), N_2F^+ (582.8), XeF^+ (689.5), NF_2O^+ (733.5) and NF_4^+ (753.5), where F^+ itself was set to zero and the value for KrF^+ was calculated from known heats of formation data. Larger F^+ detachment energies were found to correlate with decreased oxidizing power of a compound, which corresponds in this series to increasing thermodynamic stability of the N-fluorocation.

In 1994, Sudlow and Woolf described an approach based on semiempirical molecular orbital calculations for a series of N-fluoropyridinium salts and their R_3N precursors.[88] The calculated enthalpy of the "reduction couple" [ΔH_f^o (R_3N) − ΔH_f^o (R_3N^+F)] was correlated with the LUMO energy of the N-fluoropyridinium cation, where the calculated enthalpy is related to the FPD energy discussed above. A thermodynamic

ordering based on calculated F^+ detachment enthalpies, which correlated with LUMO energies of the N-fluoropyridinium ions, was proposed.

In 2016, the FPD approach was extended to 130 electrophilic N−F reagents by Cheng et al. for the construction of an energetic scale for fluorination, based on DFT calculations.[89] The fluorinating potentials of the electrophilic N−F reagents in two commonly used solvents, DCM and MeCN, were computed in terms of N−F bond heterolysis energies as expressed by the FPD values (**Equation 1**).

$$ Y\!-\!F \xrightarrow[\Delta H^o]{FPD} Y^- + F^+ \tag{1} $$
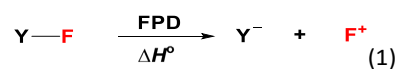
The FPD scales calculated by Cheng et al. cover a range of 469.9 to 1215.0 kJ mol⁻¹ and 464.0 to 1164.8 kJ mol⁻¹ in DCM and

MeCN, respectively (we have converted these and other values in this review to units of kJ mol^{-1} to maintain consistency). The scales comprise the *N*-fluorosulfonimides, *N*-fluorosulfonamides, *N*-fluorocarboxamides, *N*-fluoro heterocycles, *N*-fluoropyridiniums and *N*-fluoroammoniums. A scale containing several of the most commonly employed N−F reagents is shown in **Figure 4**. Lower energies correspond to increasing electrophilic fluorinating power. In MeCN, NFPy **14**, NFSI **23** and Selectfluor™ **25** were all predicted to have very similar reactivities, separated by only 0.8 kJ mol^{-1}. However, based on the synthetic literature precedent (which will be further discussed in Section 8), these reagents show very different reactivities. With DCM as the solvent, the relative reactivities were very similar, except NFSI **23** which was predicted to be less reactive than triMe-NFPy **18**. The *N*-fluoropyridinium salts cover a wider FPD range, with pentaCl-NFPy **17** predicted to have one of the highest fluorinating powers. Counterions were not specified, despite the fact that solvation and ion-pairing effects have been shown to greatly influence fluorination reactions.[77] Additionally, nucleophiles were not included in their models, so it is difficult to relate the predicted reactivities to specific substrates and their solvational requirements.
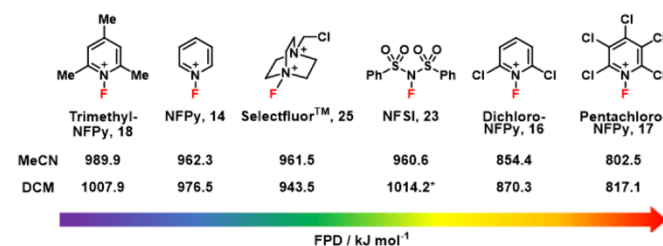

Figure 4: Selected N−F reagents and their FPD values in MeCN and DCM. Counterions were not specified. *NFSI **23** was predicted to have lower reactivity in DCM than the reagents shown.[89]

In 2019, Du *et al*. theoretically analysed the activation barriers to fluorination of benzene with 16 disubstituted *N*-fluoropyridinium tetrafluoroborate salts in MeCN using DFT.[90] The nitro-substituted salts were predicted to have the greatest electrophilicities, and within this class, the 2,6-dinitro-*N*-fluoropyridinium salt **59e** was predicted to be the most reactive (**Scheme 2**). The authors envisioned that their theoretical studies could aid in the design of more efficient *N*-fluoropyridinium salts.
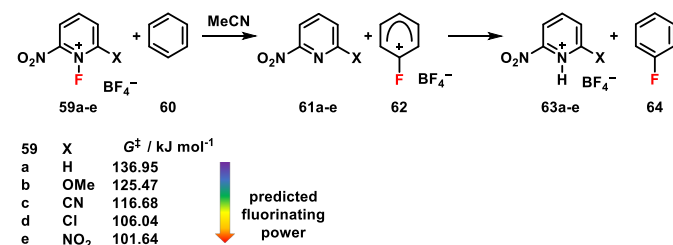

Scheme 2: Proposed mechanism and reaction energy barriers, ΔG‡, for fluorination of benzene with 2,6-di-substituted *N*-fluoropyridinium salts **59a-e**.[90]

5. Competition kinetics approaches

5.1 Competitive kinetics of fluorination of acetylenes with Selectfluor™

In 1995, Zupan *et al*.[91] examined substituent effects on the relative rates of fluorination of phenylacetylene systems using competition experiments. Studies were conducted on the four alkynes **65a-d** shown in **Scheme 3**. In a typical experiment, Selectfluor™ **25** (1 mmol) was added to a solution of the reference nucleophile (1-phenyl-1-propyne **65a**, 0.5 mmol) and the substituted alkyne (**65b-d**, 0.5 mmol). The mixture was heated to 76 °C for 10-20 h, and the consumption of substrates was monitored using KI starch paper. The mixture was worked up via extraction with water and DCM, and the resulting products were analysed by NMR spectroscopy. The fluorinations of alkylphenylacetylenes **65a-d** all followed Markovnikov regioselectivity, forming only α,α-difluoroketones **66a-d**. As shown in **Scheme 3**, phenylacetylene **65b** was at least 100 times less reactive than phenylpropyne **65a**. Substitution of a bulkier *tert*-butyl group (**65c**) slightly decreased the reactivity, while a phenyl group (**65d**) decreased the reactivity further.
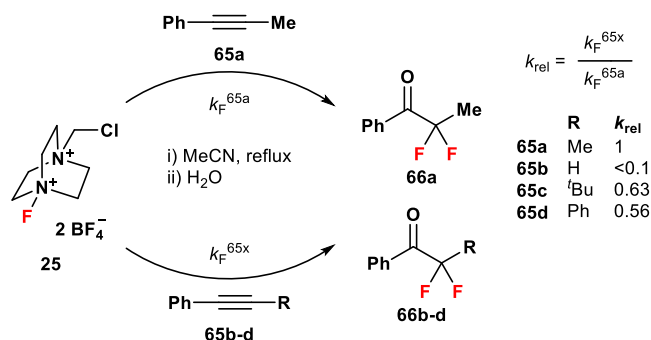
Scheme 3: Fluorination of alkylphenylacetylenes by Selectfluor™ **25** in MeCN/water under reflux. Relative rate factors were obtained via competition studies using **65b**, **65c** or **65d** in competition with 1-phenyl-1-propyne **65a**.[91]

5.2 Competitive halogenation approach

In 2004, Togni and co-workers obtained the relative rates of fluorination of a β-keto ester **67** by seven N−F reagents, in the presence of a titanium catalyst, using competitive, parallel halogenation processes (**Scheme 4a**).[92] The competition reactions were carried out in the presence of a mixture of *N*-chlorosuccinimide **68** (NCS, 1 equiv.) and the chosen fluorinating agent (1 equiv.). The catalyst [TiCl₂(TADDOLato)] **71** (where TADDOL = α,α,α′,α′-tetraaryl-2,2-dimethyl-1,3-dioxolan-4,5-dimethanol) was used to give high enantioselectivities. After full consumption of the β-keto ester **67** (1 equiv.) as determined by TLC monitoring, the composition of the resulting mixture **69/70** of α-halogenated β-keto esters was determined by chiral HPLC. The authors assumed that all the chlorination reactions occurred with the same rate constant (k_{Cl}) in parallel to the competing fluorination processes. The molar ratios of the two halogenated products were considered as relative measures of the rates of fluorination with each N−F reagent, as described by **Equation 2**, where k_F and k_{Cl} are the bimolecular rate constants for fluorination and chlorination,

respectively. The parameters n_F and n_{Cl} represent the experimentally measured molar amounts of fluorination and chlorination products formed, respectively. Such "clock" reactions are a well-established strategy for the determination of rate constants for direct reactions of carbocations with nucleophiles, for example, Jencks used bisulfite[93] and azide[94] ions to trap carbocations. Normally, large excesses of both electrophiles are used to ensure first-order behaviours with respect to both electrophiles throughout the reaction course.

$$k_{rel}(\text{F/Cl}) \; = \; \frac{k_F}{k_{Cl}} = \frac{n_F}{n_{Cl}} \qquad (2)$$

The k_{rel}(F/Cl) values were calculated from the ratios of products at the end-point of the reactions as determined by chiral HPLC (**Table 2**). The combined yield of fluorinated products in each reaction was divided by that of the chlorinated products to give the k_{rel}(F/Cl) values listed in the table. According to the results, Selectfluor™ **25** and Accufluor™ **27** are the most powerful fluorinating agents. The N-fluoropyridinium salts **16b**, **29** and **30** showed moderate to low reactivities. The neutral amine derivatives reacted slowly; for example, NFSI **23** reacted 70 times slower than Selectfluor™ **25**, while perfluoropiperidine **8** was the least reactive reagent towards β-ketoester **67** (see **Table 2**).

A computational study on the mechanism of fluorination of β-ketoester **67** in the presence of the Ti catalyst **71** was reported,[95] where it was proposed that binding of the dicarbonyl to the catalyst leads to the formation of complex **72-enolate** that immediately precedes what is assumed to be the (fully) rate limiting fluorination step (**Scheme 4b**). The presence of the Ti catalyst is likely to have significant effects on the rate constants of the competitive halogenations, so it is important to consider that the k_{rel}(F/Cl) values capture the relative reactivites of the fluorinating agents towards intermediate **72-enolate**, rather than the β-ketoester **67**.

Table 2: Results of competitive halogenations. Yields were determined by HPLC.[92]

Fluorinating power	N–F reagent	Product **69**		Product **70**		k_{rel}(F/Cl)
		Yield / %	ee / %	Yield / %	ee / %	
	N-Fluoro-perfluoropiperidine **8**	3	74	97	64	0.03
	NFSI **23**	4	67	96	63	0.04
	Synfluor™ **30**	6	45	94	62	0.06
	diCl-NFPy BF$_4^-$ **16b**	13	53	87	49	0.15
	NFPy-2-sulfonate **29**	45	74	55	38	0.81
	Accufluor™ **27**	65	60	35	49	1.84
	Selectfluor™ **25**	73	70	27	57	2.72
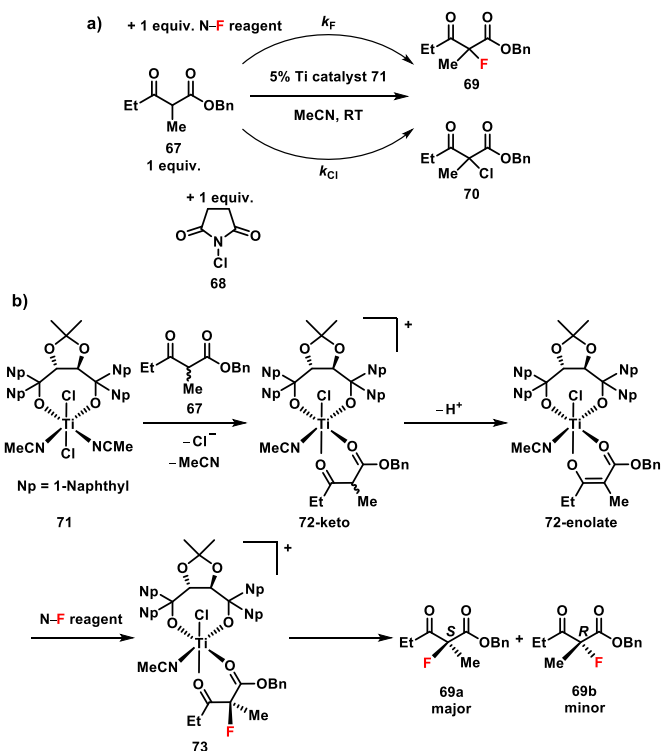
Scheme 4: (a) Competitive halogenation reaction reported by Togni et al.[92] (b) Proposed mechanism for the Ti-catalysed asymmetric fluorination reaction of a β-ketoester.[95]

6. Kinetics of fluorination of nucleophilic substrates

6.1 Kinetics of fluorination of anisole, fluorene, diphenylether, dibenzofuran, biphenyl and diphenylmethane with Selectfluor™

Beginning in 1996, Zupan, Stavber and co-workers determined the second-order rate constants for the fluorination of a range of nucleophilic substrates using Selectfluor™ **25** and Accufluor™ **27**. Firstly, the kinetics of fluorination of various aromatic compounds using Selectfluor™ **25** will be discussed. The consumption of Selectfluor™ **25** during fluorination reactions was monitored using iodometric titration to obtain kinetic data. Thermostatted, temperature-matched solutions of the nucleophile were added to solutions of the N−F reagent. After various time intervals, aliquots were removed and mixed with ice cold KI solution. The liberated iodine was then titrated with Na$_2$S$_2$O$_3$, to afford second-order rate constants.

Table 3: Summary of second-order rate constants, k_2, for the fluorination of aromatic systems by Selectfluor™ **25** in MeCN at 65 °C.[96,97]

Structure	k_2 / M^{-1} s^{-1}
Anisole **74**	4.8×10^{-3}
Fluorene **76**	3.6×10^{-3}
Diphenylether **78**	6.0×10^{-4}
Dibenzofuran **80**	2.5×10^{-4}
Biphenyl **82**	1.0×10^{-4}
Diphenylmethane **84**	6.0×10^{-5}

The rates of fluorination of anisole **74**,[96] fluorene **76**,[97] diphenylether **78**,[96] dibenzofuran **80**,[96] biphenyl **82**[96] and

diphenylmethane **84**[97] using Selectfluor™ **25** were determined in MeCN (**Table 3**). The synthetic reactions are summarised in **Scheme 5** to show regioselectivities and isolated yields. Conducting the fluorination of diphenylmethane **84** in the presence of nitrobenzene, as a radical scavenger, gave similar distributions of fluorinated products, but only 14% of the product from the oxidation process, benzophenone **85a**, was formed. This indicates that the fluorination reaction does not proceed through radical species, while the competing oxidation process may involve the formation of radical intermediates, resulting in the formation of non-fluorinated products.
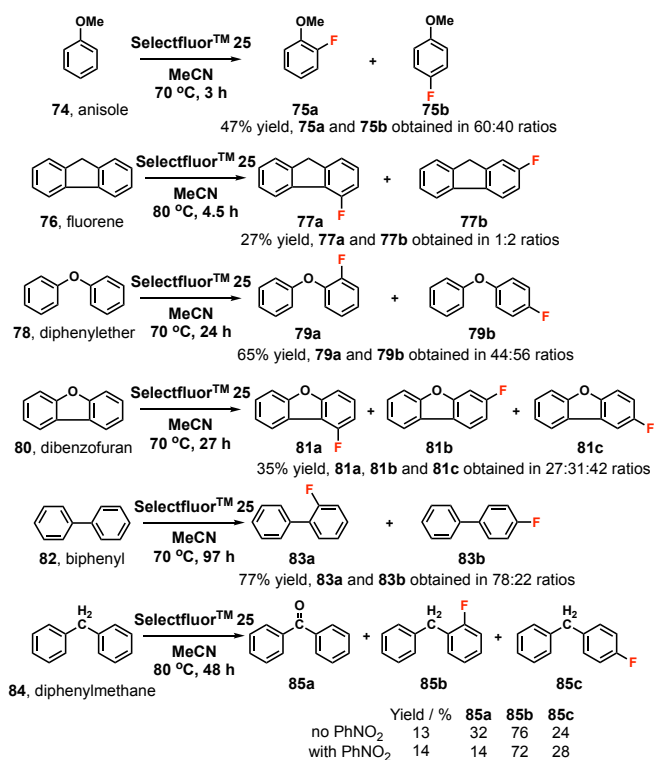

Scheme 5: Fluorination of anisole **74**,[96] fluorene **76**[97] diphenylether **78**,[96] dibenzofuran **80**,[96] biphenyl **82**[96] and diphenylmethane **84**[97] using Selectfluor™ **25**.

6.2 Kinetics of fluorination of phenyl-substituted alkenes with Accufluor™

In 2000, Stavber et al.[98] reported the kinetics of fluorination of phenyl-substituted alkenes **86a-c** and **89** with Accufluor™ **27** in MeCN at 24 °C, with MeOH as the secondary nucleophile, using the iodometric titration method (**Scheme 6**). Vicinal fluoro-methoxy adducts **88a-f** were obtained, with Markovnikov-type regioselectivities. The effects of alkene structure on the rates of fluorination are shown by the rate constants in **Table 5**. The main factor affecting the fluorination rate was the number of phenyl groups around the double bond; introduction of two or three groups into the molecule increased the reactivity of the substrate. However, the rate constant for the reaction involving tetraphenylethene **86c** was slightly lower than that of triphenylethene **86b**, which was attributed to steric factors. The use of water as the secondary nucleophile gave small reductions in k_2 values (1.3- to 2-fold, see **Table 5**). Activation parameters were also determined for the fluorination of alkene **86a**. The

$\Delta G^{\ddagger}$ values were 85 kJ mol^{-1} in the presence of each secondary nucleophile. The $\Delta H^{\ddagger}$ parameters were 74 kJ mol^{-1} in the presence of water, and 62 kJ mol^{-1} with MeOH. The $\Delta S^{\ddagger}$ values obtained were −37 J K^{-1} mol^{-1} with water, and −75 J K^{-1} mol^{-1} with MeOH. Similar activation parameters were also obtained for alkene **89** (**Table 5**). These values suggest bimolecular rate-determining steps, in both cases, with a greater entropy loss for MeOH, possibly because of a greater requirement for solvent re-organisation at the transition state in MeOH.
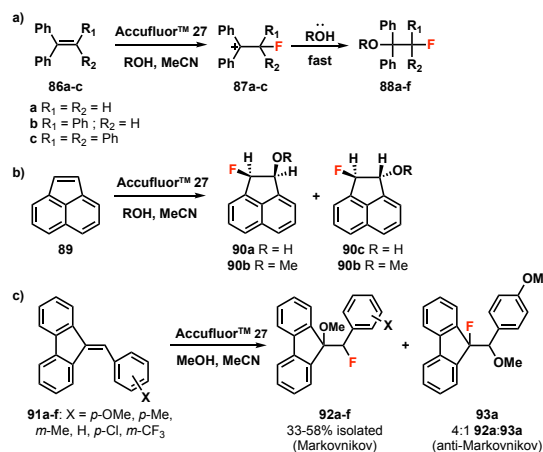
Scheme 6: Fluorination of substituted alkenes **86a-c** and **89** with Accufluor™ **27** (ROH = H$_2$O, MeOH). Reactions of 9-benzylidenefluorene derivatives **91a-f** with Accufluor™ **27** in MeOH-MeCN mixtures.

To gain further insight into the fluorination of alkenes **86a-c** with Accufluor™ **27**, the reactivities of these substrates were compared using relative rates (relative to triphenylethene) for the fluorinations of **86a-c** using XeF$_2$/HF and CsSO$_4$F.[54] The relative rates of reactions of alkenes **86a-c** with XeF$_2$/HF were very similar to those of Accufluor™ **27**, and both reagents showed increased rates as a result of additional phenyl groups. In contrast, in the case of fluorination of alkenes **86a-c** with CsSO$_4$F,[54] further introduction of phenyl groups to the alkene decreased the reactivity.

The kinetics of fluorination of 9-benzylidenefluorene **91a-f** with Accufluor™ **27** were studied (**Scheme 6c**). Substrates with substituted phenyl rings were used to investigate electronic effects upon alkene structure during the reaction. A linear Hammett correlation was obtained with a relatively small, negative constant ($\rho^+ = -0.95$) which indicated a non-polar character in the transition state. On the basis of their kinetic experiments, an S$_N$2 mechanism at the electrophilic fluorine centre was proposed, involving the formation of carbocation intermediates (analogous to **87a-c**, **Scheme 6a**). With alkene **91a**, the anti-Markovnikov product **93a** was also obtained in 4:1 ratio of **92a:93a**, as determined by NMR spectroscopy. The formation of this product was associated with the stabilising effect of the p-OMe group towards the proposed benzylic carbocation intermediate.

Many fluorination reactions have been conducted in aqueous media,[99] and Zupan et al.[100] reported the kinetics of decomposition of Selectfluor™ **25** in the presence of water, MeCN and MeOH (**Table 4**). The observed rate constant for

decomposition of Selectfluor™ **25** is highest in the presence of MeOH, which suggested that when MeOH or water are used as secondary nucleophiles, slow, competing decomposition pathways may also occur.

Table 4: Rate constants for the decomposition of Selectfluor™ **25** in water, water:MeCN 1:1 and water:MeOH 1:1, determined from iodometric titration experiments.[100]

Solvents	Temp / °C	$k_{obs} \times 10^5$ / s^{-1}
Water	60	1.1
	70	2.8
Water:MeCN 1:1	60	1.3
	70	2.4
Water:MeOH 1:1	60	3.5
	70	8.7

Table 5: Summary of second-order rate constants, k_2, and activation parameters for fluorination reactions involving substituted alkenes **86a-c, 89** and **91a-f** using Accufluor™ **27** at 24 °C.[98]

Nucleophile	Solvents (11:1 ratios)	k_2 / M^{-1} s^{-1}	$\Delta G^{\ddagger}$ / kJ mol^{-1}	$\Delta H^{\ddagger}$ / kJ mol^{-1}	$\Delta S^{\ddagger}$ / J K^{-1} mol^{-1}
86a	MeCN/MeOH	9.1×10^{-3}	85	62	−74
	MeCN/H$_2$O	6.7×10^{-3}	85	74	−37
86b	MeCN/MeOH	2.7×10^{-2}	-	-	-
86c	MeCN/MeOH	2.0×10^{-2}	-	-	-
89	MeCN/MeOH	5.5×10^{-3}	86	63	−75
	MeCN/H$_2$O	2.8×10^{-3}	88	74	−44
91a (*p*-OMe)	MeCN/MeOH	2.6×10^{-2}	-	-	-
91b (*p*-Me)	MeCN/MeOH	7.8×10^{-3}	-	-	-
91c (*m*-Me)	MeCN/MeOH	5.2×10^{-3}	-	-	-
91d (H)	MeCN/MeOH	4.7×10^{-3}	-	-	-
91e (*p*-Cl)	MeCN/MeOH	3.1×10^{-3}	-	-	-
91f (*m*-CF$_3$)	MeCN/MeOH	1.3×10^{-3}	-	-	-

Stavber *et al*. reported the kinetics of fluorination of *para*- or *meta*-substituted styrenes **94a-f** with Accufluor™ **27** in different solvent systems (**Scheme 7**) and constructed Hammett correlations.[101] The regioselectivities of the synthetic fluorination reactions had been previously reported.[37,102] Reactions conducted in MeCN resulted in the formation of vicinal fluoroacetamides **98a-f** in 70-80% isolated yields through Ritter-type reactions. When reactions were conducted in the presence of a secondary nucleophile (water, MeOH), in the case of styrenes with electron-donating substituents **94a-b**, only vicinal hydroxyfluorides **99a-b** and methoxyfluorides **100a-b** were obtained. Reactions with styrene **94c** resulted in the formation of trace amounts of fluoroacetamide **98c**, while *m*-nitrostyrene **94e** gave 50% **98e** alongside **99e** or **100e**. For reactions conducted in MeCN, correlation of second-order rate constants (**Table 6**) with substituent constants σ$^+$ gave the reaction constant ρ$^+$ = −1.48. Fluorination reactions conducted in the presence of small amounts of water and MeOH gave ρ$^+$ values of −1.52 and −1.80, respectively. Although the presence of secondary nucleophiles had generally small effects on the rates of fluorination, the build-up of charge was greatest in the rate-determining step for fluorination of styrenes in the presence of MeOH. It was proposed that, given the similarity of the ρ$^+$ values obtained with that of −2.20 for the reaction of

para-substituted styrenes with 2,4-dinitrobenzenesulfenyl chloride, which proceeds through a bridged episulfonium ion,[103] the mechanism for fluorination of the styrenes studied may involve the formation of bridged non-polar structures **96a-f**. Possible evidence for the formation of carbocation intermediates **97a-f** came from the observation that the addition of the secondary nucleophile followed Markovnikov-type selectivity. This contrasts with the observation of the opposite regioselectivity for reactions that proceed through radical intermediates, such as laser flash photolysis-generated ion-radicals of styrenes.[104]
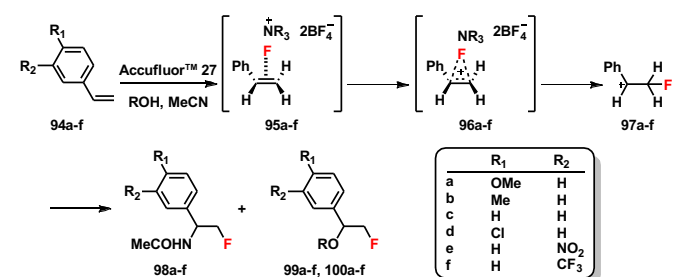
Scheme 7: Fluorination of styrenes **94a-f** with Accufluor™ **27** in MeCN, 11:1 MeCN:H$_2$O and 11:1 MeCN: MeOH. The proposed mechanism is shown. (ROH = H$_2$O, MeOH).

Table 6: Second-order rate constants for the fluorination of styrenes **94a-f** with Accufluor™ **27** at 52 °C.[101]

Nucleophile	Substituent	k_2 / M^{-1} s^{-1}		
		MeCN	MeCN:H$_2$O 11:1	MeCN:MeOH 11:1
94a	*p*-OMe	7.6×10^{-2}	6.2×10^{-2}	1.1×10^{-1}
94b	*p*-Me	1.5×10^{-2}	7.7×10^{-3}	1.4×10^{-2}
94c	H	4.5×10^{-3}	2.5×10^{-3}	3.9×10^{-3}
94d	*p*-Cl	2.2×10^{-3}	1.3×10^{-3}	2.1×10^{-3}
94e	*m*-NO$_2$	4.8×10^{-4}	2.6×10^{-4}	-
94f	*m*-CF$_3$	-	-	4.2×10^{-4}

6.3 Kinetics of fluorination of anions with NFSI

In 2000, Crugeiras *et al*.[105] reported second-order rate constants for the reaction of NFSI **23** with nucleophiles in aqueous solutions (**Table 7**). The kinetics of reactions were monitored via stopped-flow UV-vis spectrophotometry. The soft, polarizable nucleophiles I$^-$, SCN$^-$ and Br$^-$ reacted at fluorine, whereas hard oxygen and nitrogen nucleophiles reacted at sulfur. The ambient reactivity of NFSI **23** was suggested to be due to the relative contributions of electrostatic and orbital interactions. *Ab initio* single-point calculations showed that sulfur is the most electron deficient centre on the NFSI molecule, whereas the charge on the fluorine atom is close to zero. It was suggested that the addition of nucleophiles at the electrophilic fluorine site is controlled by frontier orbital interactions rather than by charge distribution, whereas nucleophilic attack at the sulfonyl group may be a charge-controlled process. With the chlorinated analogue, *N*-chlorobenzenesulfonimide (NCSI), anions reacted only at the chlorine atom. This was attributed to the lower electronegativity of chlorine compared to fluorine, and therefore the lower electrophilicity of the sulfonyl group of NCSI

than NFSI; thus, both hard and soft nucleophiles react at chlorine. Rate constants for reactions of anions with NCSI could not be determined as they were too fast to be monitored with the stopped-flow instrument. For the reaction of Br^- with NCSI (at chlorine) a value of $k_{Br} \geq 4 \times 10^5$ M^{-1} s^{-1} was estimated, which is 8 orders of magnitude greater than the rate constant for the reaction of Br^- with NFSI **23** (at fluorine).

Table 7: Kinetics of fluorination of anions I^-, SCN^- and Br^- with NFSI **23** in aqueous solutions at 25 °C. Second-order rate constants for reactions occurring at sulfur are shown for comparison. Ionic strength, I, was 1.0 using KCl.[105]

Nucleophile	Electrophilic site	k_2 / M^{-1} s^{-1}
I^-	F	66 ± 1
Br^-	F	$(2.1 \pm 0.1) \times 10^{-3}$
SCN^-	F	1.89 ± 0.06
HO^-	S	117 ± 2
N_3^-	S	0.345 ± 0.006

6.4 Kinetics of fluorination of norbornene with Selectfluor™

In 2001, Zupan *et al*. determined second-order rate constants for the fluorination of norbornene by iodometric titration (**Table 8**).[106] In MeCN, the *syn* and *anti* products **107a** and **108a** were formed in equal quantities through Ritter-type reactions (**Scheme 8**). In the presence of secondary nucleophiles (water, MeOH), additional products corresponding to **107b-c** and **108b-c** were obtained. The insensitivity of the rate constants and activation parameters for fluorination towards solvent polarity indicated that the differences in polarity between reactants and transition state species are minimal. The proposed fluorination mechanism was ionic in nature, involving the formation of a π-complex **103**, which reacts via three-centred transition state **104** to form β-fluorocarbenium ion **105**. Following a Wagner-Meerwein rearrangement to yield ion **106**, reaction with the secondary nucleophile gives the final products.

Scheme 8: Proposed mechanism for the fluorination of norbornene **102** using Selectfluor™ **25**. ROH = H_2O, MeOH.

Table 8: Kinetics of fluorination of norbornene **102** using Selectfluor™ **25**.[106]

Solvents	Temp / °C	Product distribution	$k_2 \times 10^3$ / M^{-1} s^{-1}	$\Delta H^\ddagger$ / kJ mol^{-1}	$\Delta S^\ddagger$ / J K^{-1} mol^{-1}
MeCN	20	**107a**:**108a** 50:50	-	-	-
20% H_2O in MeCN	20	**107a**:**108a**:**107b**:**108b** 22:17:25:36	3.5	-	-
17% H_2O in MeCN	20	-	3.4	59.8	−83.7
	30	-	8.2		
20% MeOH in MeCN	20	**107a**:**108a**:**107c**:**108c** 7:13:33:45	-	-	-
17% MeOH in MeCN	20	-	4.5	60.7	−79.5
	35	-	16.5		

6.5 Kinetics of fluorination of phenols with Selectfluor™

In 2002, Stavber and co-workers reported the kinetics of fluorination of phenols with Selectfluor™ **25** (**Scheme 9a**) using the iodometric titration method.[107] The *o,p*-substituted phenols **109a-c** were reacted with Selectfluor™ **25** in MeCN at 15 °C (**Scheme 9a**), yielding mixtures of 2-fluoro-cyclohexa-3,5-dienones **110a-c** and 4-fluoro-cyclohexa-2,5-dienones **111a-c** in almost equimolar proportions.[107] The rate constants are summarised in **Table 9**. The least hindered phenol **109a** was four times more reactive than the most hindered derivative **109c**. In the presence of an external nucleophile ROH (water, MeOH, ethylene glycol), regiospecific formation of non-fluorinated *para*-quinol ether products **112a-c** occurred (**Scheme 9a**).[107] The addition of MeOH resulted in small increases in k_2 values for all three phenols, while the presence of ethylene glycol and water decreased the reaction rates considerably. Activation parameters ($\Delta G^\ddagger$, $\Delta H^\ddagger$, $\Delta S^\ddagger$) were obtained for the reactions of **109a-c** with Selectfluor™ **25** in the presence of external nucleophiles (**Table 9**). $\Delta G^\ddagger$ values were around 80 kJ mol^{-1} at 15 °C for all three phenol substrates, as expected from the similar k_2 values, and they were independent of the nature of the external nucleophile. The structures of the phenol substrates had little effect on activation enthalpies $\Delta H^\ddagger$ (values ∼75 kJ mol^{-1}), whereas activation entropies $\Delta S^\ddagger$ (values ranging from −5 J K^{-1} mol^{-1} to −40 J K^{-1} mol^{-1}) depended greatly on the substrate structure and the nature of the external nucleophile.

The approach was also applied towards the determination of second-order rate constants for other *para*-substituted phenols **113a-g** (**Scheme 9b**).[108] Mixtures were obtained that included ring-fluorinated, addition, *ipso*-substitution and oxidation products. Phenols with electron-withdrawing substituents gave complex mixtures of products, where fluorinated products were present in small quantities. The reaction of Selectfluor™ **25** with **113b** in MeCN gave mainly oxidation products in high yields, whereas *p*-methoxyphenol **113c** resulted in the formation of *p*-quinone **117**. Selectfluor™ **25** and **113f** in MeCN gave **114f** and **115f** in 34:66 ratios and 55% isolated yield, and **113g** in MeCN gave **114g** and **115g** in 40:60 and 78% isolated yield. Regioselectivity data for **113a-e** were not reported. A Hammett plot constructed using rate constants for the reactions of Selectfluor™ **25** with **113a-e** in MeCN at 70 °C gave $\rho^+ = -2.3$. An excellent correlation was obtained despite

the different types of ring functionalisation across the substrates. Activation parameters were also determined and are summarised in **Table 9**. In general, higher $\Delta H^{\ddagger}$ values were obtained for fluorination processes of **113a**, **113f** and **113g** (80-86 kJ mol^{-1}) than for reactions of **113b-c**, which led to mainly oxidation products (60-68 kJ mol^{-1}).

Scheme 9: Functionalisation of phenols **109a-c**[107] and **113a-g**[108] using Selectfluor™ **25**. ROH = water, MeOH, ethylene glycol.

Table 9: Summary of second-order rate constants, k_2, and activation parameters for the functionalisation of phenols **109a-c** and **113a-g** by Selectfluor™ **25** in MeCN.[107,108] Rate constants and activation parameters for reactions of **109a-c** conducted in 9:1 MeCN:MeOH to form non-fluorinated products **112a-c** are shown for comparison.[107]

Substrate	Temp / °C	Solvent	k_2 / M^{-1} s^{-1}	$\Delta G^{\ddagger}$ / kJ mol^{-1}	$\Delta H^{\ddagger}$ / kJ mol^{-1}	$\Delta S^{\ddagger}$ / J K^{-1} mol^{-1}
109a	15	MeCN	3.5×10^{-2}	-	-	-
	15	MeCN:MeOH	3.2×10^{-2}	79 ± 2	77 ± 1	−5.0 ± 0.1
109b	15	MeCN	1.5×10^{-2}	-	-	-
	15	MeCN:MeOH	1.3×10^{-2}	81 ± 2	75 ± 1	−19 ± 1
109c	15	MeCN	9.0×10^{-3}	-	-	-
	15	MeCN:MeOH	8.2×10^{-3}	82 ± 2	73 ± 1	−33 ± 1
113a	40	MeCN	1.0×10^{-3}	-	80 ± 3	−49 ± 3
	70	MeCN	1.6×10^{-2}	-	-	-
113b	17	MeCN	3.0×10^{-2}	-	68 ± 4	−39 ± 4
	70	MeCN	2.8	-	-	-
113c	25	MeCN	4.1×10^{-2}	-	60 ± 7	−70 ± 12
	70	MeCN	1.1	-	-	-
113d	70	MeCN	1.2×10^{-3}	-	-	-
113e	70	MeCN	7.1×10^{-4}	-	-	-
113f	40	MeCN	8.7×10^{-3}	-	86 ± 2	−10 ± 0.4
113g	40	MeCN	8.6×10^{-3}	-	85 ± 2	−14 ± 0.5

Since the kinetics of fluorination reactions involving Selectfluor™ **25** and Accufluor™ **27** were not studied with the same nucleophile, and kinetics studies were conducted at different temperatures, it is difficult to compare their reactivities, and such an assessment was not attempted by Stavber and co-workers. Comparing the most and least reactive phenol (this section) and alkene (Section 6.2), the k_2 values with Selectfluor™ **25** and Accufluor™ **27** are in the same order. Accounting for the temperature differences, Selectfluor™ **25** can be estimated to be slightly more reactive. This is in agreement with the competitive halogenation study for fluorination of β-ketoester **67**, discussed in Section 5.2, where Selectfluor™ **25** was 1.5-fold more reactive than Accufluor™ **27**.

6.6 Kinetics of fluorination of mesitylene with Selectfluor™

The kinetics of fluorination of mesitylene **119** with Selectfluor™ **25** were monitored using iodometric titrations by Borodkin *et al*. in 2006.[109,110] The reactions were proposed to proceed via a σ-complex **120**. Second-order rate constants were determined according to **Equation 3** (**Table 10**). By conducting reactions at four different temperatures, activation parameters were determined to be $\Delta H^{\ddagger}$ = 86 ± 3 kJ mol^{-1} and $\Delta S^{\ddagger}$ = −24 ± 9 J K^{-1} mol^{-1}. The high value of $\Delta H^{\ddagger}$ and low absolute value of $\Delta S^{\ddagger}$ were suggested to correspond to enthalpic control of the reaction with the strong C−F bond formation occurring in the rate-determining step. Kinetic isotope effect (KIE) studies were conducted, and further mechanistic discussion will be continued in Section 9.

$$\ln\frac{[\text{Mes}]}{[\text{Selectfluor}^{\text{TM}}]} = k_2([\text{Mes}]_0 - [\text{Selectfluor}^{\text{TM}}]_0)t + \ln\frac{[\text{Mes}]_0}{[\text{Selectfluor}^{\text{TM}}]_0} \quad (3)$$

$$\text{where } k_2 = \frac{k_{\text{for}}k}{(k_{\text{rev}} + k)}$$

Table 10: Kinetics of fluorination of mesitylene **119** using Selectfluor™ **25** in MeCN.[110]

Temperature / °C	k_2 / M^{-1} s^{-1}
0	1.41×10^{-5}
31	5.67×10^{-4}
39	1.85×10^{-3}
50	5.54×10^{-3}
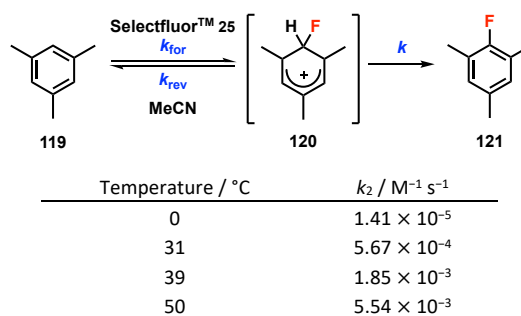
6.7 Kinetics of fluorination of uracil derivatives with Selectfluor™

In 2015, Borodkin *et al*.[111] reported kinetics studies on reactions of Selectfluor™ **25** with 6-methyluracil **122** and 1,3,6-trimethyluracil **123** in water (**Scheme 10**). With compound **122**, product ratios **124**:**126**:**128a**:**128b** of 12:7:3:68 were determined by NMR spectroscopy (2 equivalents of Selectfluor™, 40 °C, 2 h reaction time). With compound **123**, under the same conditions, product ratios **125**:**127**:**129a**:**129b** of 8:6:7:75 were obtained. Kinetics studies were conducted using iodometric titration following the method of Stavber and co-workers described in previous sections. It was determined that the fluorination reactions followed bimolecular mechanisms, according to **Equation 4**, with intermediate formation of cationic σ-complexes **A** and **B**.

$$\text{Rate} = \frac{\text{d}[\text{Selectfluor}^{\text{TM}}]}{\text{dt}} = -k_2[\text{Uracil}][\text{Selectfluor}^{\text{TM}}] \quad (4)$$
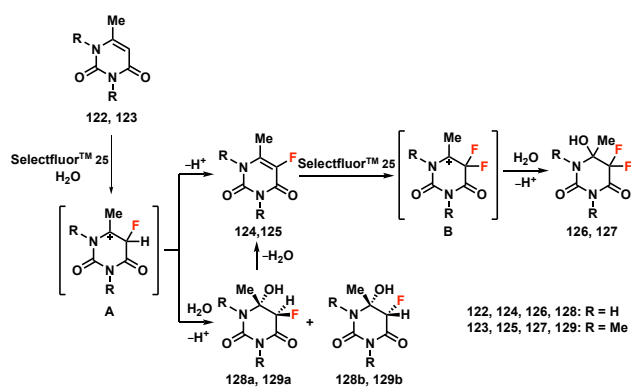
Scheme 10: Fluorination of uracils **122** and **123** using Selectfluor™ **25** in water.

Second-order rate constants for reactions conducted in water at 40 °C are summarised in **Table 11**. The higher reactivity of 1,3,6-trimethyluracil **123** compared to 6-methyluracil **122** was attributed to the electron-donating effects of methyl groups at 1- and 3-positions. The higher rate of fluorination of 5-fluoro-6-methyluracil **124** compared to 6-methyluracil **122** was rationalised by the assumed greater acidity of **124** due to the presence of a fluorine atom in the 5-position. This assumption was supported by calculated pK_a values,[112] where 5-fluorouracil was estimated to be more acidic than uracil.

Table 11: Kinetics of fluorination of uracil derivatives in water at 40 °C.[111]

Substrate	$k_2 \times 10^3$ / M^{-1} s^{-1}
6-methyluracil **122**	2.71 ± 0.03
1,3,6-trimethyluracil **123**	3.77 ± 0.03
5-fluoro-6-methyluracil **124**	4.11 ± 0.15

6.8 Kinetics of fluorination of enamines and carbanions with N−F reagents

The most extensive nucleophilicity scale currently available is the Mayr-Patz scale.[113] It was derived from the rate constants of the reactions of benzhydrilium ions with a wide range of nucleophiles including alkenes, arenes, enol ethers, ketene acetals, enamines, carbanions, amines, alcohols and alkoxides.[114] In 2018, Mayr *et al*.[115] reported a study on reactivities of five electrophilic fluorinating reagents. Kinetics studies were carried out on the reactions of enamines **130a-h** and carbanions **131a-f** (**Figure 5**) with NFPy BF$_4^−$ **14b**, diCl-NFPy BF$_4^−$ **16b**, triMe-NFPy BF$_4^−$ **18b**, NFSI **23** and Selectfluor™ **25** in MeCN using conventional and stopped-flow UV-vis spectrophotometry. Second-order rate constants determined for the fluorination reactions (**Table 12**) enabled the determination of electrophilicity parameters, E, for the N−F reagents, according to a linear free energy relationship known as the Mayr-Patz equation (**5**).[116,117] In **Equation 5**, k is the second-order rate constant at 20 °C, E is a nucleophile-independent electrophilicity parameter, and N and s_N are electrophile-independent nucleophile-specific parameters. The range of s_N values for the reference nucleophiles used in this study (0.76 to 0.86 for **130a-h** and 0.60 to 0.96 for **131a-f**) are small and do not significantly affect the interpretation of the results. The anodic peak potentials and kinetic data of the nucleophiles were used to calculate the Gibbs energies for

electron transfer, ΔG^o_{ET}, and Gibbs energies of activation for polar reactions, $\Delta G^‡_P$. Given that the $\Delta G^‡_P$ values were smaller than ΔG^o_{ET}, Mayr *et al*. concluded that the electrophilic fluorinations of the enamines proceeded via S$_N$2-type mechanisms rather than SET. Rate constants were also determined for the fluorination of nucleophiles **130d** and **131b** using the cinchona alkaloid derivative **35** (**Table 12**).

$$\log k_2 (20\,°C) = s_N(E + N) \qquad (5)$$
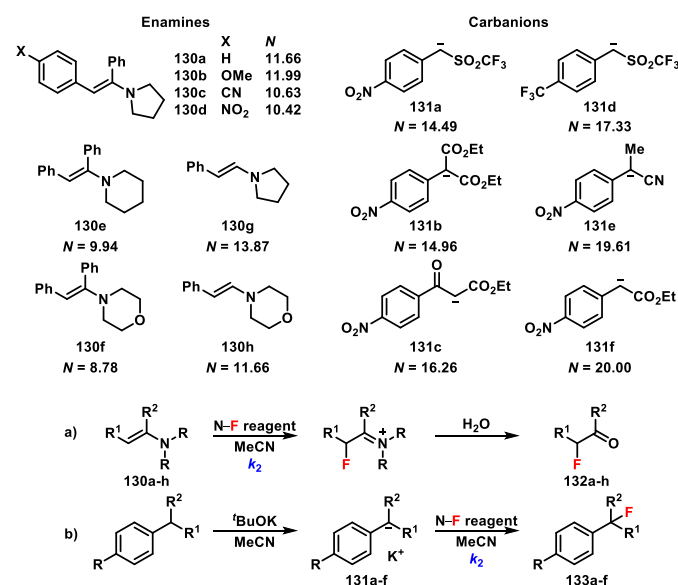
Figure 5: Structures of enamines and carbanions included in the work of Mayr *et al*.[115] for the determination of electrophilicity parameters, E, of the N−F reagents. Each nucleophile is labelled with its corresponding nucleophilicity parameter, N. N parameters for enamines **130a-h** were determined in MeCN, whereas those of carbanions **131a-f** were determined in DMSO.

Hammett correlations for enamines **130a-d** gave ρ = −0.63 for reactions involving Selectfluor™ **25** and ρ = −0.80 for those with NFSI **23**. The fact that the reactions of the N−F reagents with enamines **130** and carbanions **131** followed separate Mayr-Patz correlations attests to the use of structurally differing nucleophiles (whose nucleophilicities were determined using a homologous series of benzhydrylium ions). The possibility that these differences could be due to the nucleophilicity parameters for the carbanions that were determined in DMSO rather than MeCN was ruled out. Thus, only the enamine-derived rate constants were used to determine electrophilicity parameters, E, for the five N−F reagents (**Figure 6**). As a result, deviations of up to 4 orders of magnitude were obtained for the fluorinations of carbanions **131** using the enamine-derived E parameters to predict rate constants. The fluorinating reagents have comparable reactivities to three chlorinating reagents based on polychloroquinone structures, for which E parameters are known[118] (**Figure 6**), however, the reactivities of other halogen (Br, I) transfer reagents have not yet been quantified using the Mayr-Patz equation. The electrophilicities of 9 trifluoromethylthiolating reagents were reported by Xue *et al*. in 2018, and have E parameters from −6.06 to −23.32.[119]
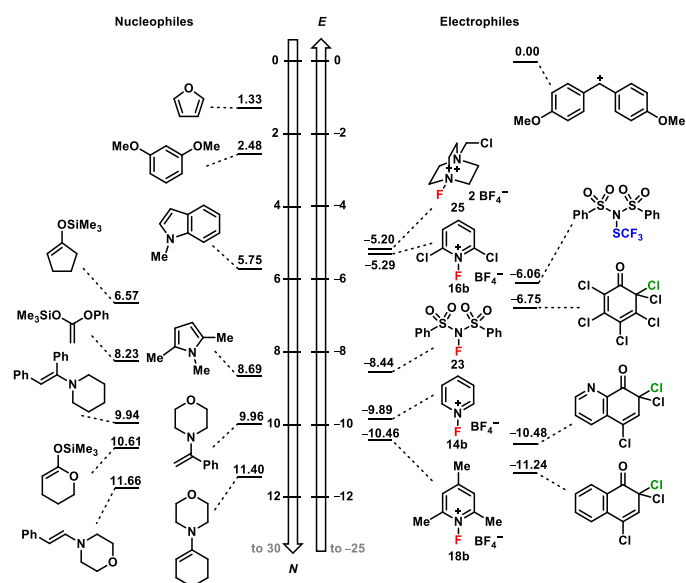
Figure 6: Scales of electrophilic and nucleophilic reactivities quantified using E parameters and N parameters. Values taken from ref.[114]

Table 12: Second-order rate constants, k_2, for the fluorination of enamines **130a-h** and carbanions **131a-f** using N−F reagents in MeCN at 20 °C (from ref. [115]).

N−F reagent	Nucleophile	k_2 (20 °C) / M^{-1} s^{-1}
NFPy BF$_4^-$ **14b**	**130a**	2.26×10^1
	130c	4.38
	130d	3.61
	130e	1.03
	130g	4.53×10^1
diCl NFPy BF$_4^-$ **16b**	**130a**	1.30×10^5
	130c	4.71×10^4
	130d	2.91×10^4
	130e	4.61×10^3
	130g	2.40×10^5
	130h	9.97×10^3
triMe-NFPy TfO$^-$ **18a**	**130a**	8.60
	131b	2.92×10^3
	131c	1.02×10^4
triMe-NFPy BF$_4^-$ **18b**	**130a**	1.08×10^1
	130c	1.68
	130e	2.62×10^{-1}
	130g	9.99
	131a	7.43×10^2
	131b	1.34×10^3
	131c	4.15×10^3
	131d	2.00×10^4
	131f	8.18×10^4
NFSI **23**	**130a**	3.00×10^2
	130b	6.13×10^2
	130c	1.17×10^2
	130d	7.41×10^1
	130e	1.11×10^1
	130f	2.72
	130g	2.42×10^2
	130h	2.38×10^1
	131a	1.29×10^2
	131b	7.71×10^2
	131c	1.02×10^3
	131d	6.28×10^2
	131e	1.27×10^4
Selectfluor™ **25**	**130a**	1.08×10^5
	130b	1.87×10^5
	130c	5.09×10^4
	130d	3.53×10^4
	130e	9.82×10^3
	130f	2.30×10^3
	130g	8.14×10^4
	130h	7.75×10^3
Cinchona alkaloid	**130d**	2.27×10^2
derivative **35**	**131b**	1.57×10^5

6.9 Kinetics of fluorination of enolic 1,3-dicarbonyl compounds with N−F reagents

Also in 2018, we reported a quantitative reactivity scale that spans eight orders of magnitude, for ten commonly-exploited N−F reagents (**Figure 7**).[120] The reactivity of each fluorinating reagent was assessed by directly monitoring the kinetics of fluorination reactions with a family of 1,3-diaryl-1,3-dicarbonyl nucleophiles **134a-m** that mirrors the applications of the reagents in C−F bond formation towards common drug

precursors (**Scheme 11**). The reactivities of the homologous nucleophiles were found to span 5 orders of magnitude, which allowed reactivity determinations to be performed in a comparative manner using NMR spectroscopy and UV-vis spectrophotometry. Second-order rate constants, k_2, were determined according to **Equation 6** and are summarised in **Table 13**.
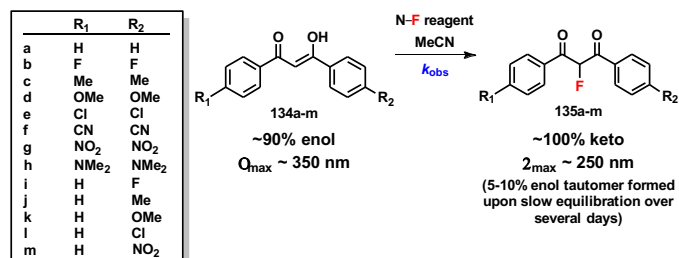
Scheme 11: Kinetics studies for mono-fluorination of **134a-m** by N−F reagents.
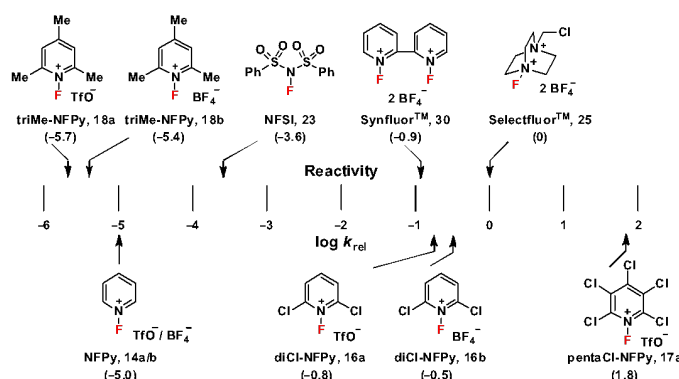
Figure 7: Quantitative reactivity scale for ten electrophilic fluorinating reagents of the N−F class, constructed using averages of the relative rate constants, determined from kinetics studies.[120]

Table 13: Second-order rate constants (k_2) and k_{rel} values for the reactions of fluorinating reagents **14a/b**, **16a/b**, **17a**, **18a/b**, **23**, **25** and **30** with nucleophiles **134a-m** in MeCN at 25 °C (from refs. [120,121]).

Nucleophile (R groups)	Electrophile	k_2 (25 °C) / M^{-1} s^{-1}	k_{rel}
134a-enol ($R_1 = R_2 = H$)	Selectfluor™ **25**	4.20×10^{-2}	1.0
	Cl$_2$-NFPy TfO⁻ **16a**	9.85×10^{-3}	2.3×10^{-1}
	Cl$_2$-NFPy BF$_4$⁻ **16b**	1.20×10^{-2}	2.9×10^{-1}
	Cl$_5$-NFPy TfO⁻ **17a**	3.53	8.4×10^1
	NFSI **23**	9.87×10^{-6}	2.4×10^{-4}
134b-enol ($R_1 = R_2 = F$)	Selectfluor™ **25**	3.28×10^{-2}	1.0
	Cl$_2$-NFPy TfO⁻ **16a**	3.35×10^{-3}	1.0×10^{-1}
	Cl$_2$-NFPy BF$_4$⁻ **16b**	1.30×10^{-2}	4.0×10^{-1}
	NFSI **23**	8.14×10^{-6}	2.5×10^{-4}
134c-enol ($R_1 = R_2 = Me$)	Selectfluor™ **25**	1.17×10^{-1}	1.0
	Cl$_2$-NFPy TfO⁻ **16a**	2.41×10^{-2}	2.1×10^{-1}
	Cl$_2$-NFPy BF$_4$⁻ **16b**	4.44×10^{-2}	3.8×10^{-1}
	Cl$_5$-NFPy TfO⁻ **17a**	5.91	5.1×10^1
	NFSI **23**	3.08×10^{-5}	2.6×10^{-4}
134d-enol ($R_1 = R_2 = OMe$)	Selectfluor™ **25**	6.43×10^{-1}	1.0
	NFPy TfO⁻ **14a**	6.90×10^{-6}	1.1×10^{-5}
	NFPy BF$_4$⁻ **14b**	6.29×10^{-6}	9.8×10^{-6}
	Cl$_2$-NFPy TfO⁻ **16a**	1.14×10^{-1}	1.8×10^{-1}
	Cl$_2$-NFPy BF$_4$⁻ **16b**	1.61×10^{-1}	2.5×10^{-1}
	Cl$_5$-NFPy TfO⁻ **17a**	2.72×10^1	4.2×10^1
	triMe-NFPy TfO⁻ **18a**	1.34×10^{-6}	2.1×10^{-6}
	triMe-NFPy BF$_4$⁻ **18b**	2.63×10^{-6}	4.1×10^{-6}
	NFSI **23**	1.38×10^{-4}	2.2×10^{-4}
	Synfluor™ **30**	6.76×10^{-2}	1.1×10^{-1}
134e-enol ($R_1 = R_2 = Cl$)	Selectfluor™ **25**	1.82×10^{-2}	1.0
	Cl$_2$-NFPy TfO⁻ **16a**	2.94×10^{-3}	1.6×10^{-1}
	Cl$_2$-NFPy BF$_4$⁻ **16b**	5.47×10^{-3}	3.0×10^{-1}
	Cl$_5$-NFPy TfO⁻ **17a**	1.42	7.8×10^1
	NFSI **23**	5.75×10^{-6}	3.2×10^{-4}
134f-enol ($R_1 = R_2 = CN$)	Selectfluor™ **25**	1.60×10^{-3}	1.0
134g-enol ($R_1 = R_2 = NO_2$)	Selectfluor™ **25**	8.99×10^{-4}	1.0
134h-enol ($R_1 = R_2 = NMe_2$)	Selectfluor™ **25**	1.05×10^2	1.0
	NFSI **23**	1.41×10^{-2}	1.3×10^{-4}
134i-enol ($R_1 = H, R_2 = F$)	Selectfluor™ **25**	3.71×10^{-2}	1.0
134j-enol ($R_1 = H, R_2 = Me$)	Selectfluor™ **25**	7.70×10^{-2}	1.0
	Cl$_2$-NFPy BF$_4$⁻ **16b**	2.39×10^{-2}	3.1×10^{-1}
	NFSI **23**	1.82×10^{-5}	2.4×10^{-4}
134k-enol ($R_1 = H$, $R_2 = OMe$)	Selectfluor™ **25**	1.89×10^{-1}	1.0
	Cl$_2$-NFPy BF$_4$⁻ **16b**	4.50×10^{-2}	2.4×10^{-1}
	NFSI **23**	4.18×10^{-5}	2.2×10^{-4}
	Synfluor™ **30**	2.44×10^{-2}	1.3×10^{-1}
134l-enol ($R_1 = H, R_2 = Cl$)	Selectfluor™ **25**	2.81×10^{-2}	1.0
134m-enol ($R_1 = H, R_2 = NO_2$)	Selectfluor™ **25**	8.86×10^{-3}	1.0

$$\text{Rate} = -\frac{\text{d[Nuc]}}{\text{dt}} = k_2[\text{Nuc}][\text{NF reagent}] \quad (\textbf{6})$$

To enable direct comparisons of reactivities, relative rate constants for the fluorination reactions were determined using **Equation 7**. Hammett plots were constructed using σ_p^+ values,

and we found that the ρ⁺ values for each fluorinating reagent were between −1.4 and −2.0 for di-substituted derivatives **134a-h** and between −0.72 and −0.83 for mono-substituted derivatives **134i-m**. These negative values indicate moderate reductions in electron density on the substrates during the rate determining fluorination steps. The similarity in each set of ρ⁺ values suggests that the fluorination mechanisms are analogous across the range of fluorinating reagents, which is a critical requirement for the construction of a predictive reactivity scale. The average k_{rel} values for each reagent were used to construct the reactivity scale in **Figure 7**. The most reactive reagent was determined to be pentaCl-NFPy TfO⁻ **17a**, which was one order of magnitude more reactive than Selectfluor™ **25**. Synfluor™ **30**, diCl-NFPy TfO⁻ **16a** and diCl-NFPy BF₄⁻ **16b** were one order of magnitude less reactive than Selectfluor™ **25**. NFSI **23**, NFPy TfO⁻/BF₄⁻ **14a/14b** and triMe-NFPy TfO⁻/BF₄⁻ **18a/18b** were four, five and six orders of magnitude less reactive than Selectfluor™ **25**, respectively. The identity of the counter-ions had small effects on the reactivities of the *N*-fluoropyridinium salts, where the tetrafluoroborate salts were generally slightly more reactive. Activation parameters (Δ$G^{\ddagger}$, Δ$H^{\ddagger}$ and Δ$S^{\ddagger}$) were obtained from kinetic data for the reactions of Selectfluor™ **25** with **134a-e** (**Table 14**). The moderately negative values of Δ$S^{\ddagger}$, taken together with the Hammett reaction constants, support an S$_N$2-type mechanism for the fluorination reactions.

$$k_{rel} = \frac{k_2(\text{NF reagent})}{k_2(\text{Selectfluor}^{TM})} \quad (7)$$

Table 14: Activation parameters for fluorinations of **134a-e**, **135a** and **135d** with Selectfluor™ **25**, determined using Eyring correlations.[120,122]

Nucleophile	σ$_p^+$	Δ$H^{\ddagger}$ / kJ mol⁻¹	Δ$S^{\ddagger}$ / J K⁻¹ mol⁻¹	Δ$G^{\ddagger}$ / kJ mol⁻¹
134a (R₁ = R₂ = H)	0	64.3	−55.8	80.9
134b (R₁ = R₂ = F)	−0.07	60.3	−71.1	81.5
134c (R₁ = R₂ = Me)	−0.31	62.2	−53.7	78.2
134d (R₁ = R₂ = OMe)	−0.78	54.8	−64.6	74.1
134e (R₁ = R₂ = Cl)	0.11	61.3	−72.3	82.9
135a (R₁ = R₂ = H)	0	60.7	−66.9	80.6
135d (R₁ = R₂ = OMe)	−0.78	53.2	−69.7	74.0

6.10 Kinetics of fluorination of enolic 2-fluoro-1,3-dicarbonyl compounds with N−F reagents

Fluorine-containing 1,3-dicarbonyl derivatives[123] and α,α-difluorocarbonyl compounds[124] are important building blocks for drug discovery and manufacture. However, difficulties have often been reported in controlling mono- versus di-fluorination of 1,3-dicarbonyl compounds, leading to challenging separations of the product mixtures. To understand the factors that determine selectivity between mono- and di-fluorination, we performed kinetics studies on keto–enol tautomerism and fluorination processes.[122] We utilized a photo-switching method for the determination of enolization rates in 1,3-diaryl-1,3-dicarbonyl derivatives **134** and their 2-fluoro analogues **135**. Reaction additives including water, acid and base accelerated

enolization processes, especially of 2-fluoro-1,3-dicarbonyl systems. Secondly, we extended our kinetics studies to determine the rates of fluorination of enolic 2-fluoro-1,3-dicarbonyls **135a,c-e** using UV-vis spectrophotometry (**Scheme 12a**, **Table 15**).[122] Activation parameters determined for fluorinations of **135a** and **135d** using Selectfluor™ **25** are included in **Table 14**. We determined that the addition of a second fluorine atom occurs at a similar or greater rate than that of the addition of the first fluorine atom, which is represented by the k_{rel}' values according to **Equation 8**. The rate-limiting step in the overall difluorination mechanism was shown to be the enolization of the mono-fluoroketo tautomer, represented by $k_{for}(F)$ in **Scheme 12b**. Our findings have important implications for the synthesis of α,α-difluoroketonic compounds, providing quantitative information to aid in the design of fluorination and difluorination reactions. The most significant was the discovery of the large acceleratory effect of the addition of water upon the enolization of the mono-fluoroketo tautomer, where the addition of significant quantities of water can be used as a simple strategy to improve difluorination using Selectfluor™ **25**. This finding has been recently supported by the synthetic work of Tang *et al*.[125]
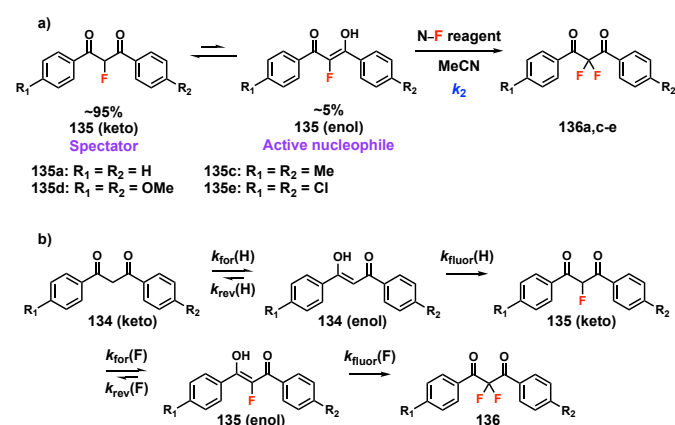
Scheme 12: (a) Kinetics of fluorination of enol tautomers of **135a** and **135c-e** using Selectfluor™ **25** and NFSI **23** in MeCN. (b) Overall mechanism for the difluorination of 1,3-dicarbonyls **134** with N−F reagents.[122]

$$k_{rel}' = \frac{k_2 (\text{addition of second fluorine atom})}{k_2 (\text{addition of first fluorine atom})} \quad (8)$$

Table 15: Second-order rate constants (k_2) for the reactions of Selectfluor™ **25** and NFSI **23** with 2-fluoro-1,3-dicarbonyls **135a** and **135c-e** in MeCN at 25 °C, and relative rates, k_{rel}', compared to the reactions of Selectfluor™ **25** and NFSI **23** with 1,3-dicarbonyls **135a** and **135c-e** according to Equation 8.[122]

Nucleophile	Electrophile	Solvents	k_2 (25 °C) / M⁻¹ s⁻¹	k_{rel}'
135a-enol	Selectfluor™ **25**	MeCN	4.37×10^{-2}	1.0
($R_1 = R_2 = H$)	Selectfluor™ **25**	MeCN	2.95×10^{-2} (20 °C)	1.1
	Selectfluor™ **25**	20% H$_2$O in MeCN	1.43 (20 °C)	57[a]
	Selectfluor™ **25**	5% formic acid in MeCN	5.35×10^{-2}	-
	NFSI **23**	MeCN	4.59×10^{-4}	46
135c-enol	Selectfluor™ **25**	MeCN	1.32×10^{-1}	1.1
($R_1 = R_2 = Me$)				
135d-enol	Selectfluor™ **25**	MeCN	6.77×10^{-1}	1.1
($R_1 = R_2 = OMe$)	Selectfluor™ **25**	MeCN	4.64×10^{-1} (20 °C)	1.1
	NFSI **23**	MeCN	6.11×10^{-4}	4.4
135e-enol	Selectfluor™ **25**	MeCN	3.07×10^{-2}	1.7
($R_1 = R_2 = Cl$)	NFSI **23**	MeCN	2.47×10^{-4}	43

[a] Fluorination of **134a-enol** in the presence of 20% water in MeCN: $k_2 = 2.49 \times 10^{-2}$.

6.11 Kinetics of fluorination of tetralone enol ester derivatives with Selectfluor™

In 2019, Nelson et al.[126] reported the kinetics of fluorination using Selectfluor™ **25** of enol ester systems based on a tetralone core (**Scheme 13**). The focus of these studies, conducted using NMR spectroscopy, was to use Hammett correlations to establish the mechanistic pathway by which fluorination occurred. From their kinetics experiments, it was concluded that an S$_N$2 reaction occurred rather than SET. ^{12}C/^{13}C kinetic isotope effect studies on compound **137a** showed that the largest KIE of 1.031 occurred at the 6-position of the tetralone core. The observed ρ⁺ values were indicative of the need for carbenium ion stabilisation. The largest ρ⁺ value (−1.36) corresponded to nucleophiles with substitution at the 6-position **137a-e**, rationalised by the extent to which the carbenium ion can be stabilised either by resonance or neighbouring group participation. The similarities in activation parameters (**Table 16**) across the enol esters indicated that a consistent mechanism was in operation for the nucleophiles that were investigated. The use of cyclopropyl-substituted substrates as radical probes gave no evidence of cyclopropyl ring-opening, thus, radical formation was ruled out. An unexpected non-fluorinated side-product **143a-f** was obtained from the fluorination reaction of **140a-f** (**Scheme 13b**), the origin of which was not fully understood. We note, however, the similarity of **143** to the products of electrochemical oxidation of a series of enol esters by Shono et al.,[127] such as α-acetoxycyclohexanone **147b** in **Scheme 13d**. Thus, since Selectfluor™ **25** is a known oxidant,[128] it is likely that the non-fluorinated side products **143a-f** may result from the oxidation of **140a-f** through a pathway that competes with the fluorination reaction.

Table 16: Activation parameters (in kJ mol⁻¹) determined via NMR spectroscopy for the fluorination of enol ester nucleophiles using Selectfluor™ **25**.[126]

Nucleophile	$\Delta G^{\ddagger}$ / kJ mol⁻¹	$\Delta H^{\ddagger}$ / kJ mol⁻¹	$\Delta S^{\ddagger}$ / J K⁻¹ mol⁻¹
137a	92.0	62.8	−100
140c	91.6	64.9	−88
144a	90.4	64.9	−84
144b	92.0	62.3	−100
144g	93.3	64.9	−96
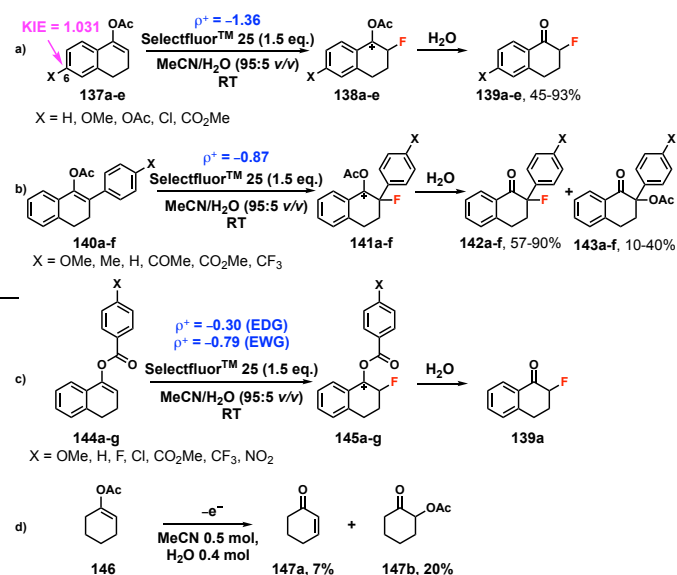
Scheme 13: (a-c) Kinetics of fluorination of tetralone derivatives using Selectfluor™ **25** by Nelson et al.[126] Isolated yields are shown. (d) Anodic oxidation of 1-cyclohexenyl acetate **146** in MeCN/H$_2$O by Shono et al.[127] Supporting electrolyte was Et$_4$NOTs.

6.12 Kinetics of fluorination of naproxen with Selectfluor™

Naproxen **148** is a nonsteroidal anti-inflammatory drug, prescribed to relieve pain, fever and swelling (**Scheme 14**). The rate of fluorination of naproxen with Selectfluor™ **25** was monitored by ^{1}H NMR spectroscopy in CD$_3$CN-D$_2$O (95:5 v/v) by Borodkin et al. in 2019.[129] The kinetics supported a bimolecular mechanism, and k_2(25 °C) was determined to be (2.42 ± 0.04) × 10^{-2} M⁻¹ s⁻¹. The formation of difluoride **149b** was proposed to occur via the monofluoride **149a**, involving trace amounts of water in the solvent. Indeed, with water as the reaction solvent, difluoride **149b** was obtained as the major product. With 2.2 equivalents of Selectfluor™ **25** in MeCN, the conversion to **149b** increased to 80%.
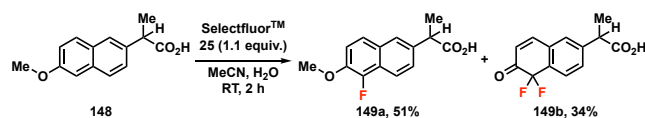
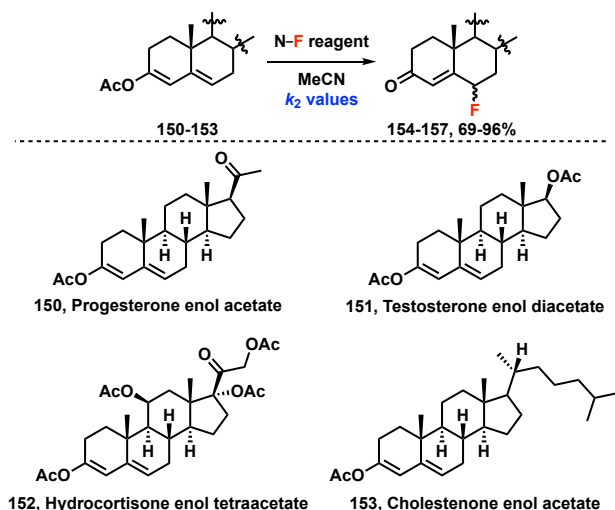Scheme 14: Kinetics of fluorination of naproxen **148** using Selectfluor™ **25**.

The use of TEMPO as a trap to detect the possible formation of cation radicals in the reaction were not successful. TEMPO, added under standard reaction conditions, resulted in the formation of approximately 5% product. As concluded by Nelson et al.,[126] the reaction between Selectfluor™ **25** and TEMPO results in the oxidation of TEMPO, so it is not suitable as

a radical trap for reactions involving this fluorinating reagent (see further discussion in Section 9).

6.13 Kinetics of fluorination of steroidal enol esters with N−F reagents

In 2020, we extended our physical organic studies to investigate the kinetics of fluorination of steroidal nucleophiles.[130] Fluorinated steroids form a significant proportion of marketed pharmaceuticals. It is estimated that 80% of manufactured fluorosteroids, marketed under tradenames such as Flixonase, Flixotide, Flonase, Flovent HFA (GSK) and Advair Diskus (GSK), are produced using electrophilic fluorinating agents such as Selectfluor™ **25**.[44] To gain quantitative information on fluorination at the 6-position of steroids, we conducted kinetics studies on enol ester derivatives of progesterone, testosterone, cholestenone and hydrocortisone **150**-**153** with a series of electrophilic N−F reagents (**Scheme 15**, **Table 17**).[130] The results correlate well with our reactivity scale, discussed in Section 6.9, thus highlighting the successful predictive power of our scale towards a different class of carbon nucleophiles (**Figure 8**).

The effects of additives, including methanol and water, upon fluorination rates of progesterone enol acetate **150** were explored. There was little variation in second-order rate constants, k_2, upon addition of 10-50% methanol (v/v in MeCN). With water, fluorination rate constants, k_2, decreased as the amount of water was increased. With 30% water in MeCN (v/v), the rate of fluorination decreased 4-fold compared with the analogous reaction in MeCN. We therefore concluded that the use of these additives offers no advantage to this particular fluorination process. Activation parameters (**Table 18**) were also consistent with those we obtained from fluorination of 1,3-dicarbonyl derivatives, thus, the fluorinations of the enol and enol ester substrates we have studied proceed via S_N2 mechanisms, but with differing solvation dependencies.

Figure 8: Correlation of log(k_{rel}) values for fluorination reactions of enol **134d** versus those of progesterone enol acetate **150**.

Table 17: Rate constants (k_2) for the fluorination of steroid enol acetates **150**-**153** by N−F reagents in MeCN or MeCN-d_3 at 25 °C. The k_{rel} values were determined using Equation 7.[130]

Nucleophile	Electrophile	k_2 (25 °C) / M^{-1} s^{-1}	k_{rel}
Progesterone enol acetate **150**	Selectfluor™ **25**	2.38	1.0
	NFSI **23**	3.33×10^{-4}	1.4×10^{-4}
	NFPy TfO⁻ **14a**	2.08×10^{-5}	8.7×10^{-6}
	triMe-NFPy TfO⁻ **18a**	7.19×10^{-6}	3.0×10^{-6}
	diCl-NFPy TfO⁻ **16a**	4.72×10^{-1}	2.0×10^{-1}
	diCl-NFPy BF$_4$⁻ **16b**	5.03×10^{-1}	2.1×10^{-1}
	pentaCl-NFPy TfO⁻ **17a**	1.31×10^{2}	5.5×10^{1}
Testosterone enol diacetate **151**	Selectfluor™ **25**	2.11	1.0
	diCl-NFPy TfO⁻ **16a**	4.41×10^{-1}	2.1×10^{-1}
	pentaCl-NFPy TfO⁻ **17a**	1.42×10^{2}	6.7×10^{1}
Cholestenone enol acetate **152**	Selectfluor™ **25**	3.18	1.0
	pentaCl-NFPy TfO⁻ **17a**	1.94×10^{2}	6.1×10^{1}
Hydrocortisone enol tetraacetate **153**	Selectfluor™ **25**	1.06	1.0
	pentaCl-NFPy TfO⁻ **17a**	5.54×10^{1}	5.2×10^{1}

Table 18: Activation parameters for the fluorinations of progesterone enol acetate **150** with Selectfluor™ **25** and diCl-NFPy TfO⁻ **16a**.[130]

N−F reagent	$\Delta G^{\ddagger}$ / kJ mol^{-1}	$\Delta H^{\ddagger}$ / kJ mol^{-1}	$\Delta S^{\ddagger}$ / J K^{-1} mol^{-1}
Selectfluor™ **25**	+71	+51	−66
diCl-NFPy TfO⁻ **16a**	+75	+52	−76

7. Comparisons of quantitative studies of fluorinating reagent reactivities

In this section, we present comparisons of the data generated by the various experimental approaches towards quantification of the reactivities of N−F fluorinating reagents. For each comparison, the logarithm of the measured rate constants, log k_2, for the reactions of N−F reagents with the 1,3-dicarbonyl **134d-enol** (R$_1$ = R$_2$ = OMe) against the corresponding literature parameters will be presented and the trends discussed. **134d-**

Scheme 15: Kinetics of fluorination of enol acetates **150**-**153** using N−F reagents to obtain the corresponding 6-fluorosteroids as mixtures of α and β isomers. Isolated yields are shown.
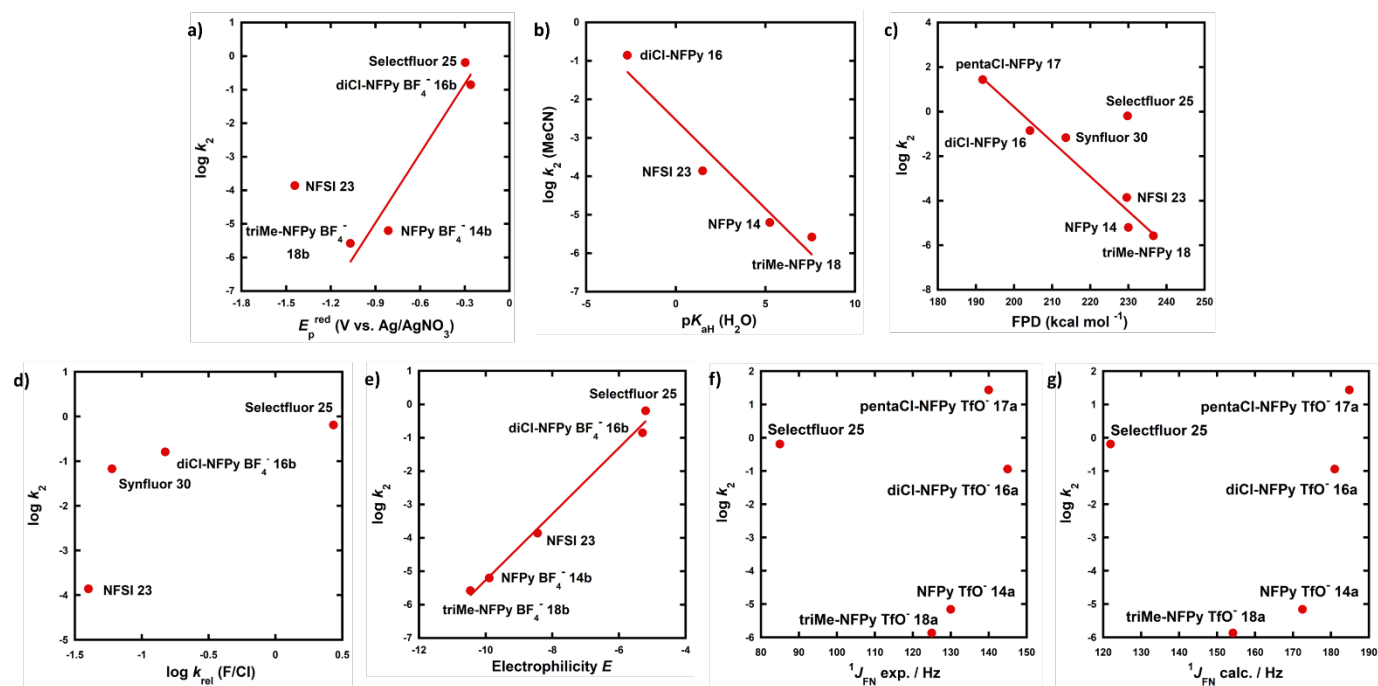
Figure 9: Plots of measured rate constants log k_2 for the reactions of N−F fluorinating reagents with **134d-enol** in MeCN at 25 °C (values from ref. [120]) against: (a) the corresponding cathodic peak potentials E_p^{red} vs. Ag/AgNO$_3$ in MeCN (values from ref. [83]; NFSI **23** is not included in the line of best fit); (b) the acidities of the corresponding N−H compounds (conjugate acids) in water (values from ref. [131]); (c) the corresponding FPD values calculated in MeCN (values from ref. [89]), Selectfluor™ **25** was not included in the correlation; (d) k_{rel}(F/Cl) values determined from competition experiments (taken from ref. [92]); (e) E parameters of five N−F reagents determined using enamines in MeCN (taken from ref. [115]); (f) experimental $^1J_{FN}$ coupling constants of the N−F reagents (taken from ref. [41]); (g) calculated $^1J_{FN}$ coupling constants of the N−F reagents (B3LYP, taken from ref. [132]).

Enol was selected for these comparisons since it has the most extensive dataset, where second-order rate constants were determined for the reactions of this compound with ten N−F reagents.[120] Furthermore, we believe our series of tuneable *C*-nucleophiles offers the most robust framework for such comparisons based on the structural homogeneity across the series. This compares with Mayr's use of tuneable benzhydrylium ions as probes for electrophilicity.

Comparing the rate constants for fluorination of **134d-enol** with the E_p^{red} values reported by Evans *et al*.,[83] NFPy BF$_4^-$ **14b**, diCl-NFPy BF$_4^-$ **16b**, triMe-NFPy BF$_4^-$ **18b** and Selectfluor™ **25** generally correlate linearly with the corresponding reduction potentials (**Figure 9a**). NFSI **23** deviates significantly from the correlation. Additionally, although the reduction potential for Selectfluor™ **25** is slightly lower than that of diCl-NFPy BF$_4^-$ **16b**, Selectfluor™ **25** is a more reactive fluorinating reagent than **16b** based on the k_2 values.

Figure 9b shows a good correlation between the reactivities of NFPy **14**, NFSI **23**, diCl-NFPy **16** and triMe-NFPy **18** with the basicities of the nucleofugal leaving groups, represented via their conjugate acid pK_{aH} values (from ref. [131]). The N−H conjugate acid of diCl-NFPy **16** is the strongest acid; therefore, its conjugate base has the lowest basicity. Weaker bases are usually better leaving groups, when making comparisons within structurally homologous series, hence, diCl-NFPy **16** was expected to be the strongest fluorinating reagent according to its aqueous pK_{aH} value. However, once again, care must be taken in correlating nucleofugality with thermodynamic parameters such as acid dissociation constants, especially when relatively few organic solvent-based pK_{aH} values are available

(e.g. only the pK_{aH} values of 2,4,6-trimethylpyridine and pyridine have been measured in MeCN[133]).

As discussed in Section 4, Christe and Dixon used enthalpies for the heterolytic cleavage of N−F reagents (fluorine plus detachment energies, FPD) as a measure for the oxidizing strengths of so-called "oxidative fluorinators".[87] Cheng *et al.* extended the work by calculating the FPD values for 130 fluorinating reagents of the N−F class.[89] The reactivities of the *N*-fluoropyridinium salts generally correlate linearly with their FPD values (**Figure 9c**). However, Selectfluor™ **25**, which was not included in the line of best fit, deviates significantly from the correlation. This deviation is likely due to the lower intrinsic barrier for reactions occurring at N(sp^3) centres compared with those at N(sp^2) centres. Intrinsic barriers for reactions occurring at DABCO and quinuclidine N(sp^3) centres have been shown to be around 40 kJ mol^{-1}, while those at DMAP N(sp^2) were around 60 kJ mol^{-1}.[134,135] In other words, there is a lower activation barrier for Selectfluor™ **25**, which is dicationic, to form a monocation than it is for NFSI **23**, a neutral compound, to form an anion upon loss of the fluorine atom. This illustrates the pitfalls of using thermodynamic methods for the estimation of a kinetic parameter such as electrophilicity. The intrinsic barrier, $\Delta G_0^{\ddagger}$, for the reduction of *N*-fluorosultam **21** was determined by Andrieux *et al.* to be 1030 meV.[86] This value converts to 99 kJ mol^{-1} and is in line with the experimental $\Delta G^{\ddagger}$ values summarised in Section 6 for reactions of Selectfluor™ **25**, Accufluor™ **27** and diCl-NFPy TfO$^-$ **16a**, once account is taken of a thermodynamic driving force component, which will lead to a lower experimental value than for the isoergic $\Delta G_0^{\ddagger}$ intrinsic process.

According to the relative reactivities determined by Togni *et al*.[92] via competitive halogenations, Selectfluor™ **25** reacted 18-fold faster than diCl-NFPy BF$_4^-$ **16b**, 45-fold faster than Synfluor™ **30** and 68-fold faster than NFSI **23**. Therefore, although the overall trend in reactivities is the same as that obtained from kinetics studies with 1,3-dicarbonyl derivatives, the magnitudes of the relative reactivities are different (**Figure 9d**). The k_2 values determined for 1,3-dicarbonyls **134a-m** and steroids **150**-**153** showed that Selectfluor™ **25** is 4-fold more reactive than diCl-NFPy BF$_4^-$ **16b**, 10-fold more reactive than Synfluor™ **30** and around 4 orders of magnitude more reactive than NFSI **23**. As previously discussed, competition reactions by Togni *et al*. were conducted in the presence of a Ti catalyst, and the k_{rel}(F/Cl) values capture the halogenation processes of catalyst-bound substrates.

The plot of log k_2 of **134d-enol** versus the electrophilicity parameters, *E*, determined by Mayr *et al*.[115] gives excellent correlation (**Figure 9e**). Hence, rate constants derived from reactions of both enols **134** and enamines **130** are in good agreement regarding the fluorinating strengths of the N−F reagents. Since the second-order rate constants for fluorinations of steroidal enol esters **150**-**151** also showed excellent correlation with those of the enol **134d** (Section 6.13, **Figure 8**), the reactivities of N−F reagents determined in our kinetics studies and those of Mayr *et al*. are, importantly, demonstrably and quantitatively consistent across three nucleophile families. Furthermore, through this comparison, we are able to make a link to Mayr's nucleophilicity scale. Ideally, a more direct link could be formed through reactivity studies of our homologous series of dibenzoylmethane-based enol systems with Mayr's homologous series of benzhydrylium ions.

The $^1J_{(F-N)}$ coupling constants for N−F reagents were determined by Gouverneur *et al*.[41] using 2D ^{19}F–^{15}N heteronuclear correlation experiments, thus serving as a new signature for the N−F bond. The data obtained by Gouverneur *et al*. were compared with our rate constant data (**Figure 9f**). The coupling constants do not correlate with the reactivities, although some correlation is observed for *N*-fluoropyridinium series, NFPy TfO$^-$ **14a**, diCl-NFPy TfO$^-$ **16a** and triMe-NFPy TfO$^-$ **18a**.

DFT protocols were used by Saielli[132] to calculate the one-bond $^1J(^{15}$N–^{19}F) spin-spin coupling constants (SSCC) in MeCN of fluorinating reagents NFPy **14**, diCl-NFPy **16**, pentaCl-NFPy **17**, triMe-NFPy **18**, Selectfluor™ **25**, two analogues of **39**, and the ethano-Tröger's base-derived reagent **40**. Positive values for $^1J(^{15}$N$−^{19}$F) spin-spin coupling constants were determined for the SSCC values, whereas the previous study by Gouverneur *et al*.[41] assumed negative signs. The SSCC values showed good correlation with the N−F bond lengths of the compounds, however, there was no correlation with the reactivities of the N−F reagents that we have reported (**Figure 9g**). The author concluded that a correlation between SSCC values and reactivity was not expected, since reactivity is influenced by the transition state energy of the fluorination reaction, whereas the coupling constant is determined only by the molecular structure of the reagent.[132]

A comparison of the reactivities of N−F reagents bearing different counterions can also be made. For fluorination reactions in MeCN involving diCl-NFPy **16** with enols **134a-e**, diCl-NFPy BF$_4^-$ **16b** was 1.2, 3.9, 1.8, 1.4 and 1.9-fold, respectively, more reactive than the diCl-NFPy TfO$^-$ **16a**.[120] With progesterone enol acetate **150**, **16b** was 1.1-fold more reactive than **16a**.[130] Fluorination of enol **134d** using triMe-NFPy BF$_4^-$ **18b** was 2.0-fold faster than that of triMe-NFPy TfO$^-$ **18a**.[120] For enamine **130a**, the fluorination reaction was 1.3-fold faster using **18b** than with **18a** in MeCN.[115] Conversely, the fluorinations of carbanions **131b** and **131c** in MeCN were 2.2 and 2.5-fold, respectively, faster with **18a** than **18b**.[115] Umemoto *et al*.[77] reported that solvation and ion-pairing effects greatly influenced the conversions in reactions of a model silyl enol ether with *N*-fluoropyridinium salts bearing BF$_4^-$, TfO$^-$, SbF$_6^-$ and ClO$_4^-$ counterions. NFPy TfO$^-$ **14a** led to the highest conversion levels, and this was suggested to be due to its greater solubility in MeCN coupled with a lower tendency to ion pair in low-polarity solvents. Overall, the results from kinetics and synthetic studies suggest that the nature of the nucleophile also plays a role in the reactivities of N−F reagents bearing triflate and tetrafluoroborate counterions.

The absolute rate constants reported in the various kinetics studies with Selectfluor™ **25** and Accufluor™ **27** give a measure of the reactivities of the different nucleophile systems (**Figure 10**). Given that Selectfluor™ **25** and Accufluor™ **27** have similar predicted reactivities, the rate constants associated with their fluorination reactions are comparable. The *N* parameter for
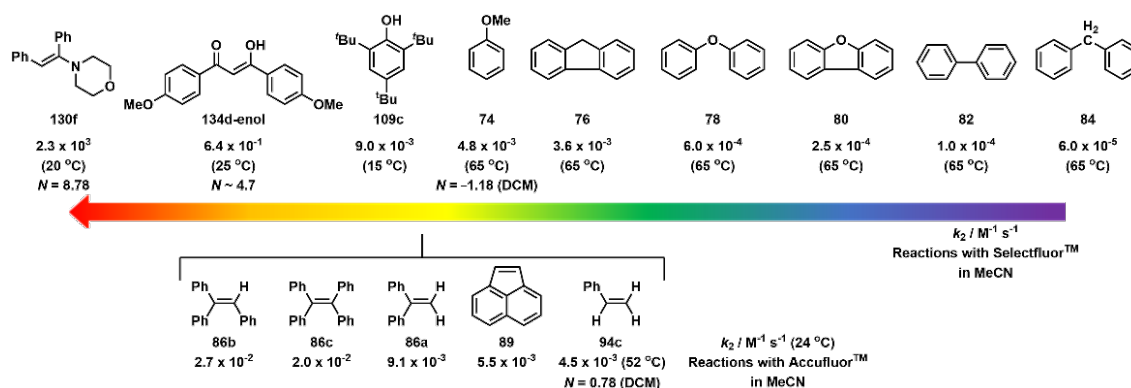

Figure 10: The nucleophilicities of several substrates based on the rate constants associated with their fluorination reactions with Selectfluor™ **25** and Accufluor™ **27**. The *N* parameter for **134d-enol** was estimated using Error! Reference source not found.**e** and **Equation 5**. For the other nucleophiles, *N* parameters were obtained from ref.[113] in MeCN,

134d-enol can be estimated from **Figure 9e** and the Mayr-Patz equation (**Equation 5**) to be $N \sim 4.7$,[121] and the N parameters for anisole **74** and styrene **94c** are known.[114] The second-order rate constants for fluorination of nucleophiles **74**, **94c**, **130f** and **134d-enol** correlate with the known or estimated N parameters.

8. Qualitative reactivities in synthetic studies

There are numerous reports in the literature where trial-and-error approaches were employed to find the most appropriate N−F reagent for specific desired transformations. Comparison of the quantitative studies discussed in Section 6 with such reports can give a good indication of the applicability of kinetic reactivity data towards synthetic studies.

In 2016, Sato *et al.*[136] reported the fluorination of 3,5-diphenylisoxazole **158** using a range of N−F reagents for reaction optimisation (**Table 19**). Under the same conditions, the reaction with Selectfluor™ **25** gave the fluorinated product **159** in 38% yield, while 2,6-diCl-NFPy TfO⁻ **16a** gave a yield of 33%. With NFSI **23**, only trace amounts of fluorination occurred, and when NFPy BF₄⁻ **14b** and 2,6-diMe-NFPy TfO⁻ **160** were used, no product was detected. From these studies, Selectfluor™ **25** was identified as the most suitable N−F reagent to carry forward in further optimisations. Since all reactions were conducted under the same conditions, it is possible to make genuine comparisons between yields obtained and reactivities of the N−F reagents. The yields of fluorinated products in these synthetic experiments align excellently with our reactivity scale (**Figure 7**) and that of Mayr (**Figure 6**). Selectfluor™ **25** and 2,6-diCl-NFPy TfO⁻ **16a** have similar reactivities, although the reaction with Selectfluor™ **25** gave a slightly higher yield of product **159**; this agrees with our reactivity scale, which predicts slightly higher reactivity for Selectfluor™ **25**. NFSI **23** is the next most reactive reagent according to the reaction yields, while NFPy BF₄⁻ **14b** and 2,6-diMe-NFPy TfO⁻ **160** were seen to give the lowest yields, which correlates with the predictions of lower reactivities from our reactivity scale.

Table 19: Fluorination of 3,5-diphenyl-4-fluoroisoxazole **158** using N−F reagents. Conversions were determined by ¹⁹F NMR spectroscopy with benzotrifluoride as the internal standard.[136]
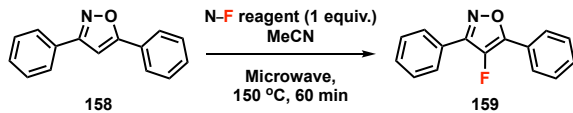
Entry	N−F reagent	Conversion to **159** / %
1	Selectfluor™ **25**	38
2	2,6-diCl-NFPy TfO⁻ **16a**	33
3	NFSI **23**	Trace
4	NFPy BF₄⁻ **14b**	nd
5	2,6-diMe-NFPy TfO⁻ **160**	nd

Reaction conditions are, however, a significant factor in fluorination reactions, as illustrated in a study by Yoshifuji et al.[137] Fluorination of azulene **161** was achieved using reagents

14a/b and **18a/b** to yield 1-fluoroazulene **162a** as the major product, in addition to small quantities of 1,3-difluoroazulene **162b** (**Table 20**). Low yields were explained, firstly, by the sensitivity of fluoroazulenes to heat, which leads to the formation of brown tar. Secondly, competing processes were reported to initiate polymerisation reactions, resulting in deep green-coloured precipitates. In a later study by Liu et al., with Selectfluor™ **25** as the fluorinating reagent, 1-fluoroazulene was obtained in 34% yield after 5 minutes at room temperature (**Table 20**, entry 6).[138] The higher yield of **162a** in this case is likely due to a combination of the higher reactivity of Selectfluor™ **25**, as well as milder conditions which reduced the amount of decomposition.

Table 20: Fluorination of azulene **161**.[137,138]
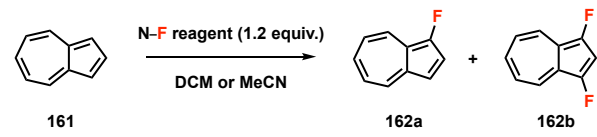
Entry	N−F reagent	Conditions	Yield / %	
			162a	**162b**
1	triMe-NFPy TfO⁻ **18a**	MeCN, reflux, 30 min	12	5
2	triMe-NFPy TfO⁻ **18a**	DCM, reflux, 45 min	17	3
3	triMe-NFPy BF₄⁻ **18b**	MeCN, reflux, 30 min	16	8
4	NFPy TfO⁻ **14a**	MeCN, 60 °C, 60 min	11	5
5	NFPy BF₄⁻ **14b**	MeCN, 60 °C, 60 min	9	6
6	Selectfluor™ **25**	MeCN:MeOH 1:5, RT, 5 min	34	3

In 2019, a team at Takeda Pharmaceutical Company reported the direct regioselective monofluorination of *N*-protected pyridone derivatives using several N−F reagents (**Table 21**).[139] The fluorination of **163** was initially performed in MeCN for 1 h at 60 °C using Selectfluor™ **25**, giving a complex mixture of products containing trace amounts of the desired 4-monofluoro-substituted product **164a** (**Table 21**, entry 1). The reaction was then performed at room temperature for 16 h, which gave product **164a** in 5% yield alongside a mixture of side-products (entry 2). These initial reactions suggested that "Selectfluor™ **25** shows extremely high reactivity toward **163** and that controlling its reactivity is difficult." Based on our quantitative studies,[120] they explored the use of reagents of differing reactivities, such as Synfluor™ **30**, NFSI **23** and triMe-NFPy TfO⁻ **18a**, to suppress the overreaction they had observed when using Selectfluor™ **25**.[139] The use of Synfluor™ **30** (entry 3) gave a complex mixture of products, while NFSI **23** (entry 4) regioselectively gave the 4-monofluorinated product **164a** in 33% yield. The use of 2.0 equiv. of NFSI **23** (entry 5) increased the yield to 50% without the generation of any side-products. However, triMe-NFPy TfO⁻ **18a** (entry 6) did not react with pyridone **163** after 12 h, likely due to its significantly lower reactivity in comparison to the other N−F reagents. Additionally, a nucleophilic fluorinating reagent, 4-*tert*-butyl-2,6-dimethylphenylsulfur trifluoride (Fluolead™) was tested, but no reaction was observed after 12 h. With the identification of NFSI

23 as the best fluorinating reagent, a range of reaction solvents was then screened, including DMF, MeOH and HFIP, although it was found that MeCN gave **164a** in the highest yield. The use of MeOH as the solvent resulted in the formation of compound **164b** instead of **164a** (**Table 21**), through nucleophilic capture of the intermediate fluoro-iminium ion. Elevated temperatures and longer reaction times resulted in the decomposition of **164a**. The substrate scope was then increased to a range of other substituted pyridones using the optimised conditions, which delivered the corresponding 4-monofluorinated products in yields of 22-51%. Selectfluor™ **25** appears to be too reactive and incompatible with the pyridone system, and the relatively high oxidising strength of this reagent is also likely to have resulted in the formation of side-products from oxidation reactions. Synfluor™ **30** is highly moisture sensitive,[120,140] and this is a possible explanation for the mixture of side-products observed. NFSI **23** is the weakest known oxidant among the N−F reagents that were trialled, and it appears to be well-matched in terms of both reactivity and selectivity towards the pyridone systems. Overall, this study shows good correlation with our reactivity scale, as well as its successful synthetic application within the pharmaceutical industry.

Table 21: Fluorinating reagents used for the monofluorination of pyridone **163**.[139]

Entry	N−F reagent (equiv.)	Time / h	Isolated yield of **164a** / %
1	Selectfluor™ **25** (1.1)	1	a
2[b]	Selectfluor™ **25** (1.1)	16	5
3	Synfluor™ **30** (1.1)	1	a
4	NFSI **23** (1.1)	1	33
5	NFSI **23** (2.0)	1	50
6	triMe-NFPy TfO⁻ **18a** (1.1)	12	No reaction
7	Fluolead™	12	No reaction

[a] Mixture of products containing trace amounts of desired product **164a**. [b] Reaction was conducted at RT.

Barbas and co-workers used α-fluoro carbonyl compounds as nucleophiles, via enamine intermediates, in aldol and Mannich-type reactions catalysed by enzymes, catalytic antibodies and organocatalysts.[141] The α-fluorination of 2-phenylpropionaldehyde **165** was carried out using five N-F reagents, in the presence of L-proline as the catalyst, in MeCN at room temperature (**Table 22**).[141] The reactions involving Selectfluor™ **25** and Accufluor™ **27** both gave high isolated yields, but afforded low *ee* values. With NFPy BF₄⁻ **14b**, no reaction occurred after 5 days, due to its low reactivity. Synfluor™ **30** gave 7% yield after 5 days, which could be due to both the reagent's sensitivity to traces of water, as reported by Umemoto[140] and in our previous studies,[120] and competing hydrolysis of enamine intermediates, brought about by the hygroscopic nature of Synfluor™ **30**. NFSI **23** was the only fluorinating reagent to give both high yield and

enantioselectivity over 24 hours. Here, NFSI **23** shows practicable reactivity towards aldehyde substrates in the presence of an organocatalyst, and this is also mirrored by its many synthetic applications in metal catalysed reactions.[142,143]

Table 22: The α-fluorination of aldehyde **165** using N−F reagents (1.2 equiv.). All isolated yields were determined after aqueous workup; enantiomeric excess was determined by chiral GLC analysis.[141]

Entry	N−F reagent (equiv.)	Time / h	Isolated yield of **166** / %	*ee* / %
1	Selectfluor™ **25**	24 h	87	4
2	Accufluor™ **27**	24 h	90	0
3	NFSI **23**	24 h	87	25
4	NFPy BF₄⁻ **14b**	5 d	NR	-
5	Synfluor™ **30**	5 d	7	12

In 2020, Cornella *et al*.[144] reported the electrophilic fluorination of arylboronic esters enabled by bismuth redox catalysis. The reactivities of several N−F reagents with phenylbismine **167** were investigated (**Table 23**). Analyses of crude reaction mixtures after reaction times of 2 h by ¹⁹F NMR spectroscopy showed only traces of fluorobenzene **168** with less reactive reagents NFPy BF₄⁻ **14b** and triMe-NFPy BF₄⁻ **18b**. With the slightly more reactive NFSI **23**, **168** was obtained in 11% yield. Selectfluor™ **25** resulted in only 7% yield of **168**. With 2,6-diCl-NFPy BF₄⁻ **16b**, which is around 3-fold less reactive than Selectfluor™ **25**, fluorobenzene **168** was obtained in 88% yield. The higher conversion with diCl-NFPy BF₄⁻ **16b** than with Selectfluor™ **25** was explained by the high lability of the neutral and sterically encumbered 2,6-dichloropyridine ligand in intermediate **169** (**Scheme 16**). Following coordination of the NCF₃ moiety, intermediate **170** eliminated fluorobenzene **168** and formed the corresponding bismine **171**. For comparison, reductive elimination with XeF₂ gave fluorobenzene **168** in 94% yield after 6 h.
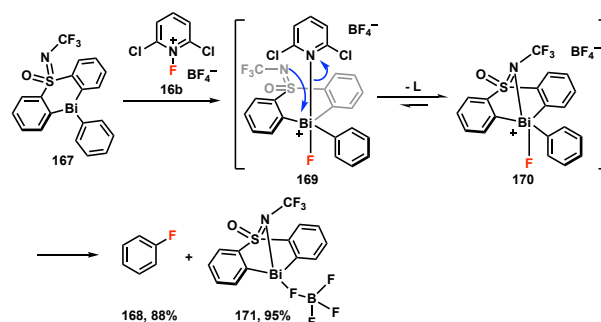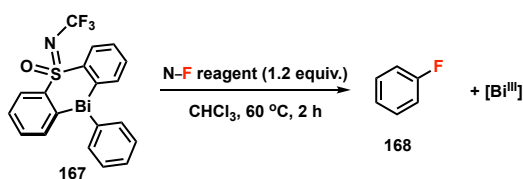

Scheme 16: Proposed mechanism for the reaction of phenylbismine **167** with 2,6-diCl-NFPy BF₄⁻ **16b** to obtain fluorobenzene **168**.[144]

Table 23: The reactions of N−F reagents with phenylbismine **167** to obtain fluorobenzene **168**.[144] Yields were determined by ^{19}F NMR spectroscopic analysis of crude reactions using 1-fluoro-4-nitrobenzene as an internal standard.

Entry	N−F reagent (equiv.)	Yield of **168** / %
1	Selectfluor™ **25**	7 [a]
2	2,6-diCl-NFPy BF$_4^-$ **16b**	88
3	NFSI **23**	11
4	NFPy BF$_4^-$ **14b**	Traces
5	triMe-NFPy BF$_4^-$ **18b**	Traces
6	XeF$_2$	94 [b]

[a] CHCl$_3$/MeCN 5:1. [b] 1.0 equiv. of XeF$_2$, 0 °C, CHCl$_3$ then 110 °C for 6 h.

9. Approaches towards the determination of the mechanism of fluorination by N–F reagents

The mechanism of so-called electrophilic fluorination has been the subject of much ongoing debate, with Eric Banks writing of a "substrate-dependent mechanistic continuum [S$_N$2(F) ↔ fully developed SET process]".[81] In 1991, Differding conducted radical-clock experiments involving reactions of a citronellic ester enolate with three N–F fluorinating reagents (*N*-fluoroquinuclidinium triflate **12**, *N*-fluorosultam **21**, and NFSI **23**) and XeF$_2$.[145] The absence of fluorinated cyclisation products, which could occur only via radical intermediates, indicated that free radicals with half-lives greater than that of the probe were not intermediates on the pathway to fluorinated products (**Scheme 18a**). Differding concluded that any observed radical intermediates are formed in a reaction competing with fluorine transfer, leading to non-fluorinated products, rather than lying on the reaction path which leads to fluorinated products. However, electron transfer followed by fast in-cage recombination was not excluded. The observed rate constants were then compared with those expected for SET processes, and it was concluded that electrophilic fluorinations of silyl enol ethers, malonate ion and enolate ions with the *N*-fluorosultam reagent **21** proceeded by direct nucleophilic attack at fluorine.[146] The extent to which competing electron transfer reactions could occur would, therefore, depend on redox potentials and reorganisation energies of the reaction partners.

In 1999, Wong *et al.*[147] investigated the reactions of vinyl ethers with Selectfluor™ **25** using a cyclopropyl radical probe (**Scheme 18b**). Products of cyclopropane ring-opening were not observed, leading to the conclusion that SET processes were not likely to be occurring. Further discussions of mechanistic studies conducted in the 1990s were included in a review by Wong *et al.* in 2005.[148] As mentioned in Section 6.11, Nelson *et al.*[126] used cyclopropyl-substituted tetralone derivatives **180** and **183** to probe the involvement of radical species, whereby a radical formed close to the cyclopropyl group would lead to ring-

opening (**Scheme 18c**). No ring-opened products were in evidence; thus, the involvement of radical species was excluded.

The kinetics of fluorination of mesitylene **119** with Selectfluor™ **25** were discussed in Section 6.6. In addition, the kinetic isotope effects in electrophilic fluorination of aromatic compounds, including mesitylene, benzene and naphthalene, using NFSI **23**, Selectfluor™ **25** and Synfluor™ **30**, were reported by Borodkin *et al.* in 2007.[109] The small values of k_H/k_D (0.86-1.00), estimated by GC-MS and NMR spectroscopy techniques, supported a polar reaction mechanism, with non-rate-limiting deprotonation of the Wheland intermediate, thus implying rate-limiting fluorination. Quantum chemical calculations (using the method reported by Stewart[149]) for the reaction of mesitylene **119** with Selectfluor™ **25** were consistent with a polar mechanism involving the formation of a σ-complex.[109]

The relative reactivities of durene and mesitylene have been used as a mechanistic probe to differentiate between SET and S$_N$2 mechanisms in electrophilic aromatic substitution reactions, including iodination, bromination and acetylation.[150] Laali and Stavber have reported that SET mechanisms are expected to be dominant for reactions of durene, while a two-electron transfer mechanism is expected for reactions of mesitylene (**Scheme 17**). In 2002, Laali reported that the competitive fluorination of mesitylene and durene with Selectfluor™ **25** in MeCN and ionic liquid gave k_{Mes}/k_{Dur} = 6 and 10, respectively.[151] These data were interpreted in terms of a polar mechanism involving the formation of a σ-complex, with a slightly greater degree of polar character developing in the ionic liquid solvent. Similar competition studies by Stavber *et al.* in 2006 reported the higher reactivity of durene than mesitylene (k_{Mes}/k_{Dur} = 0.24) towards Selectfluor™ **25** in aqueous MeCN.[152] Therefore, a SET process was proposed to be the dominant mechanism, involving the formation of a π-complex between the alkylbenzene and the N–F reagent, followed by single electron transfer to a cation radical. The competitive fluorinations of mesitylene and durene with NFSI **23** under solvent-free reaction conditions were investigated by Borodkin *et al.* in 2009.[153] NFSI **23** and substrates mesitylene and durene were mixed at a molar ratio of 1:5:5, and heated for 35 min at 105 °C, followed by analysis by ^{19}F NMR spectroscopy. The rate constant ratio k_{Mes}/k_{Dur} was estimated to be 3.4, indicating that the reaction follows a polar mechanism.
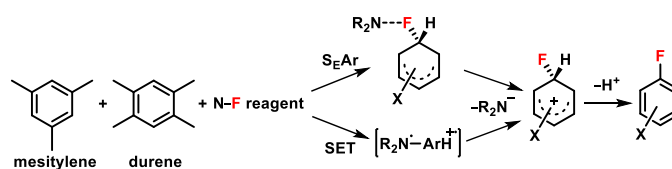
Scheme 17: Competitive fluorination reaction with mesitylene and durene, used as a mechanistic probe.
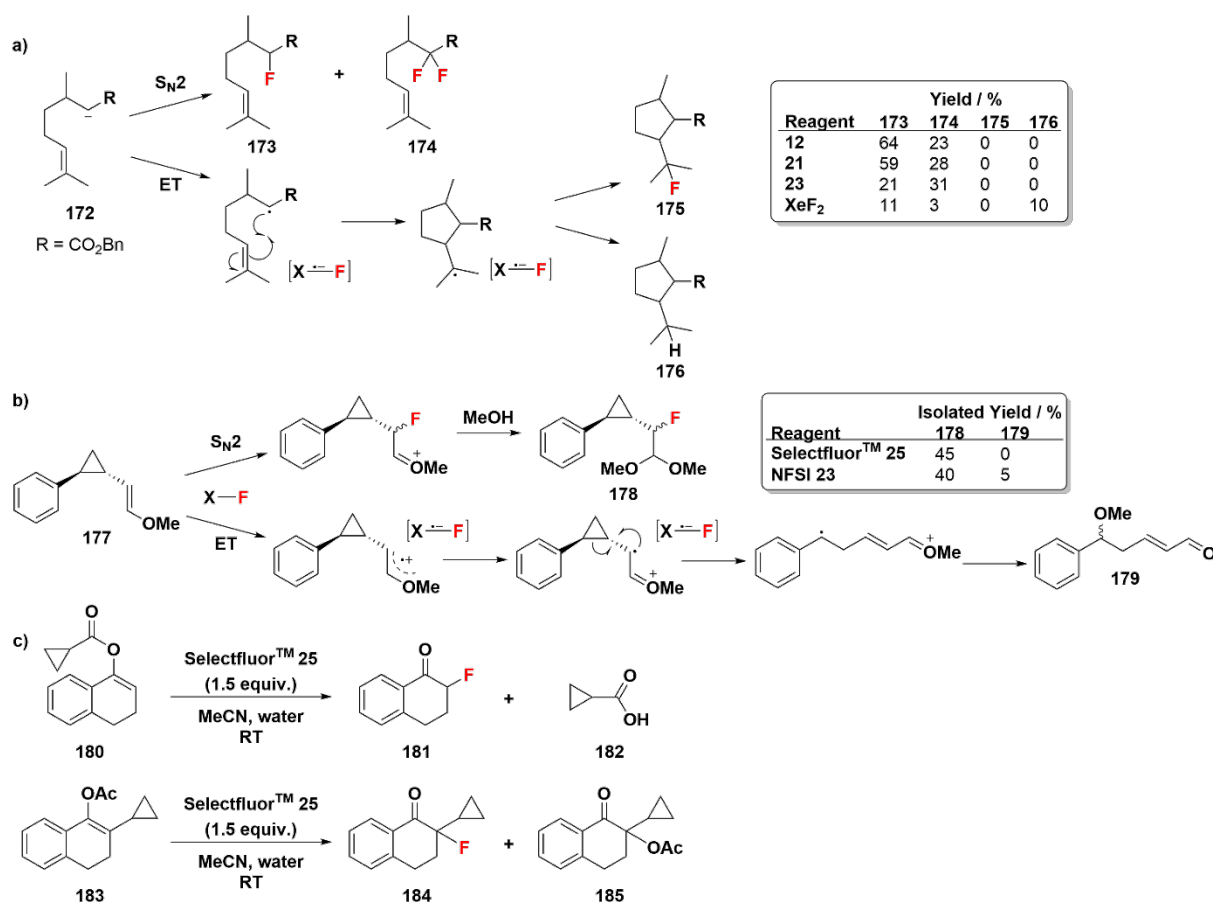
Scheme 18: Radical trapping experiments. (a) Reaction of a citronellic ester enolate derivative with electrophilic fluorinating reagents.[145] (b) Reaction of a cyclopropyl radical probe with N−F reagents.[147] (c) Reaction of cyclopropyl-substituted tetralone derivatives with Selectfluor™ **25**.[126]

In 2015, the fluorinations of aromatic compounds, including fluorobenzene, benzene, toluene and aniline, were studied theoretically by Liu *et al*.[154] Lower energy barriers were found for single-electron transfer from the aromatic substrate to Selectfluor™ **25** compared with the S_N2 mechanism, with energy differences of 17-38 kJ mol^{-1} (calculated in both gas phase and in MeCN). It was proposed that an F…π bond contributes to the stabilization of the π complex.

Gómez-Suárez *et al*.[155] have recently, in 2020, reviewed the synthetic applications of the radical dication, TEDA$^{2+•}$ (*N*-(chloromethyl) triethylenediamine), which may be generated from Selectfluor™ **25** after electron or fluorine transfer steps, usually in metal- or light-mediated processes. For example, in 2014, Lectka *et al*.[156] reported copper-catalysed monofluorination reactions accompanied by formation of TEDA$^{2+•}$. This reaction was investigated using radical clock experiments, kinetic isotope effect studies, UV-vis analyses and DFT. In 2016, Lectka *et al*.[157] proposed the formation of *N*-centred radicals generated from one-electron reduction of the N−F reagent and concomitant loss of F$^-$ initiated by direct photoexcitation. In 2019, Togni *et al*.[158] reviewed the chemistry of pyridinium salts as functional group transfer reagents and they suggest that such reagents can react via radical mechanisms due to their high oxidative strengths.

Several synthetic-scale thermal and photoinduced fluorinations, recently reviewed by Postigo *et al*.,[159] have been proposed to proceed via radical mechanisms. Hierso *et al*. have reviewed the mechanisms of palladium-catalysed electrophilic C−H fluorination.[160] The aminofluorination of a styrene with NFSI **23** was reported by Liu *et al*. where the radical scavengers 2,4-dinitrophenol or 1,3-hydroquinone had no effect on reactions, thus ruling out radical mechanisms.[161]

Several groups have attempted to probe the mechanisms of fluorination by Selectfluor™ **25** using the radical scavenger 2,2,6,6-tetramethylpiperidin-1-yloxyl (TEMPO) (**Scheme 19**), although recent findings have shown that TEMPO is oxidised by Selectfluor™ **25** and is an unreliable radical trap. In 2016, Chen *et al*.[162] reported that the electrophilic fluorination of **186** using Selectfluor™ **25** gave the product **187** in 91% yield, while the reaction conducted in presence of TEMPO (2 equiv.) gave 68% isolated yield of the fluoride product **187** (**Scheme 19a**). Possible TEMPO adducts were not found in the reaction mixture. The authors concluded that SET processes were not occurring; instead, an ionic mechanism was proposed. Also in 2016, Tang *et al*.[163] reported the decarboxylative fluorination of cinnamic acids with Selectfluor™ **25**. When TEMPO was added to the reaction, the expected product **189** was not detected (**Scheme 19b**). The authors stated that "this result indicates that
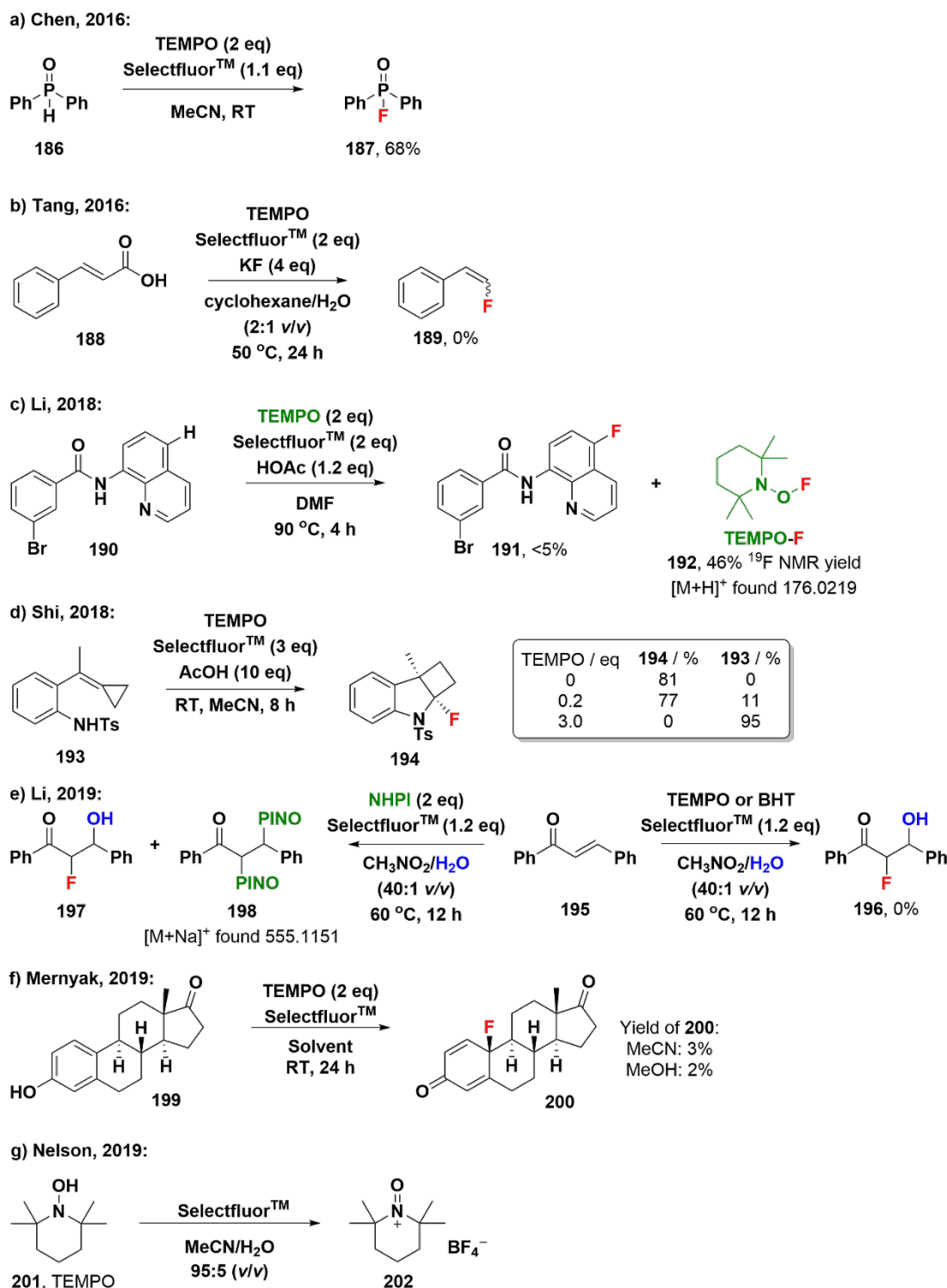
Scheme 19: Reactions of Selectfluor™ **25** in the presence of radical scavengers.

a free radical pathway might be involved in this transformation."

In 2018, Li *et al*.[164] reported the C–H fluorination of 8-aminoquinoline amide derivatives with Selectfluor™ **25**. The addition of TEMPO to a reaction resulted in the detection of <5% yield of the desired fluorinated product **191** (**Scheme 19c**). The adduct TEMPO-F **192** was obtained in 46% yield,

determined by ^{19}F NMR spectroscopy, and HR-MS analysis confirmed its formation. Shi *et al*.[165] reported the intramolecular gem-aminofluorination of *ortho*-sulfonamide-tethered alkylidene-cyclopropanes. The addition of catalytic amounts of TEMPO gave a reduced yield of the expected product **194** and recovery of the starting material **193** (**Scheme 19d**). The use of 3 equivalents of TEMPO led to recovery of the

starting material **193** and decomposition of Selectfluor™ **25**, as detected by HR-MS. Li *et al.*[166] also reported in 2019 that the α-fluoro-β-hydroxylation and α-fluoro-β-amidation of chalcone **195** were inhibited by TEMPO or 2,6-di-*tert*-butyl-4-methylphenol (BHT) (**Scheme 19e**). When another radical scavenger, *N*-hydroxyphthalimide (NHPI) was tested, analysis of the crude product by HR-MS revealed the presence of the radical addition product **198**. In 2019, Mernyak *et al.*[167] reported the fluorination of 13β-estrone **199** using Selectfluor™ **25** in MeCN to obtain 10β-fluoroestra-1,3-den-3-one **200** in 95% yield (**Scheme 19f**). However, in the presence of TEMPO, the reaction was inhibited, with only 3% yield of fluorosteroid **200**. Based on the studies involving radical scavengers, SET fluorination processes were proposed in the latter five cases (**Scheme 19b-f**). In 2019, Nelson *et al.*[126] reported that the reaction between Selectfluor™ **25** and TEMPO **201** led to the formation of oxoammonium salt **202**, as identified by comparison of IR and UV spectra with those of an authentic sample of **202** prepared by reaction of TEMPO with bleach and tetrafluoroboric acid (**Scheme 19g**). Importantly, the authors concluded that the use of TEMPO as a radical trap in reactions involving Selectfluor™ **25** is unreliable. This result was subsequently confirmed by Borodkin *et al.*[129]

In summary, several strategies have been attempted to determine the mechanisms of fluorination reactions, including radical trapping, mesitylene/durene competitive fluorinations, addition of radical scavengers and KIE studies. Selectfluor™ **25** can react through SET mechanisms, as evidenced by its reaction with TEMPO (**Scheme 19g**). In the case of electrophilic fluorination, the lifetime of the fluorine radical, if formed at all, is too short, and the radicals react faster than rates of diffusion (absolute rate constant for reaction of the laser flash photolysis-generated F• with solvent is 10^9-10^{11} s^{-1}).[168]
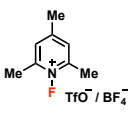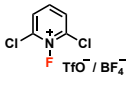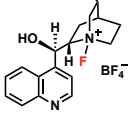
10. Summary of all kinetic reactivity studies, conclusions and outlooks

Table 24 summarises the quantitative kinetic findings of several research groups that were discussed in the preceding sections. The first kinetics studies were conducted by Zupan and Stavber between 1995-2006. These were followed by the work of Crugeiras in 2000, and Borodkin and co-workers between 2006-2019. Over the last three years, our work and those of Mayr and Nelson groups have added significantly to the field.

Table 24: Summary of all kinetics studies discussed in this review.

N–F reagent	Nucleophiles	Parameters obtained	References
	Phenyl-substituted acetylenes	k_{rel} values from NMR conversions	Zupan *et al.*[91]
Selectfluor™ 25	β-Ketoester	k_{rel} from competitive halogenations	Togni *et al.*[92]
	Anisole, fluorene, biphenyl, diphenylether, dibenzofuran, diphenylmethane	k_2 values, activation parameters	Stavber *et al.*[96,97]
	Norbornene	k_2 values	Zupan *et al.*[106]
	Phenols	k_2 values, activation parameters	Stavber *et al.*[107,108]
	Mesitylene	k_2 values	Borodkin *et al.*[110]
	Uracils	k_2 values	Borodkin *et al.*[111]
	Enamines, carbanions	k_2 values, E parameters	Mayr *et al.*[115]
	Enolic 1,3-dicarbonyl derivatives	k_2 values, Hammett correlations, activation parameters	Hodgson *et al.*[120,122]
	Tetralone derivatives	Hammett correlations, activation parameters	Nelson *et al.*[126]
	Naproxen	k_2 value	Borodkin *et al.*[129]
	Steroid enol esters	k_2 values, activation parameters	Hodgson *et al.*[130]
NFSI 23	β-Ketoester	k_{rel} from competitive halogenations	Togni *et al.*[92]
	I$^-$, SCN$^-$ and Br$^-$	k_2 values	Crugeiras *et al.*[105]
	Enamines, carbanions	k_2 values, E parameter	Mayr *et al.*[115]
	Enolic 1,3-dicarbonyl derivatives	k_2 values, Hammett correlations	Hodgson *et al.*[120,122]
	Steroid enol esters	k_2 values	Hodgson *et al.*[130]
Accufluor™ 27	β-Ketoester	k_{rel} from competitive halogenations	Togni *et al.*[92]
	Phenyl-substituted alkenes	k_2 values, activation parameters, Hammett correlations	Stavber *et al.*[98]
NFPy 14a/b	Enamines, carbanions	k_2 values, E parameter (**14b**)	Mayr *et al.*[115]
	Enolic 1,3-dicarbonyl derivatives	k_2 values (**14a/b**)	Hodgson *et al.*[120]
	Steroid enol esters	k_2 values (**14a**)	Hodgson *et al.*[130]
	Enamines, carbanions	k_2 values, E parameter (**18b**)	Mayr *et al.*[115]
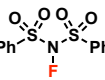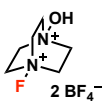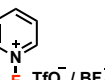
Reagent	Nucleophile	Measurement	Reference
triMe-NFPy 18a/b	Enolic 1,3-dicarbonyl derivatives	k_2 values (18a/b)	Hodgson et al.[120]
	Steroid enol esters	k_2 values (18a)	Hodgson et al.[130]
diCl-NFPy 16a/b	β-Ketoester	k_{rel} from competitive halogenations (16b)	Togni et al.[92]
	Enamines, carbanions	k_2 values, E parameter (16b)	Mayr et al.[115]
	Enolic 1,3-dicarbonyl derivatives	k_2 values (16a/b)	Hodgson et al.[120]
	Steroid enol esters	k_2 values, activation parameters (16a/b)	Hodgson et al.[130]
pentaCl-NFPy 17a	Enolic 1,3-dicarbonyl derivatives	k_2 values, Hammett correlations	Hodgson et al.[120]
	Steroid enol esters	k_2 values	Hodgson et al.[130]
Synfluor™ 30	β-Ketoester	k_{rel} from competitive halogenations	Togni et al.[92]
	Enolic 1,3-dicarbonyl derivatives	k_2 values	Hodgson et al.[120]
Cinchona alkaloid derivative 35	Enamine, carbanion	k_2 values	Mayr et al.[115]

Electrophilic fluorinating reagents of the N−F class are widely employed in both research laboratory- and industrial production-scale reactions. In recent years, the quantification of the reactivities of these reagents has been achieved with a range of nucleophilic substrates using physical organic techniques. Nucleophiles have included aromatic systems, alkenes, acetylenes, enamines, 1,3-dicarbonyl derivatives and enol esters. Independent kinetics studies conducted by our group and the Mayr group have provided consistent rankings of the reactivities of the most commonly used N−F reagents. Additional comparisons with computational, mechanistic and synthetic reports show greater or lesser levels of correlation, depending on the nature of the studies and the factors that are, or are not, taken into account. Recent studies have given clear evidence in support of S_N2-type transfer of fluorine from electrophilic N−F sources to nucleophilic substrates, under metal catalyst-free and non-photocatalytic conditions.

Across the broader fluorination chemistry field, the development and application of several classes of fluorinating reagents are being increasingly accompanied by kinetic or mechanistic understanding. Works by Jones on the Rupert-Prakash reagent (TMSCF₃),[169,170] trifluoromethylation chemistry by Schoenebeck[171–173] and hydrogen bonded phase-transfer catalysis with CsF by Gouverneur[174] exemplify this. Future directions across the field are likely to continue in this vein. A key challenge in the development of novel electrophilic fluorinating reagents is to balance their reactivity against their persistence and shelf-stability. Developing lower molecular weight reagents for more atom economical processes is another challenge. A combination of computational, kinetic and synthetic studies is likely to play a key role in the development of new reagents by design. We hope that the summarised absolute and relative rate constants, activation parameters, Hammett reaction constants and electrophilicity E parameters included in this review will serve as a useful resource for informing reagent choice, the design of new fluorinating reagents, and the general enhancement of fluorination reactions through greater quantitative understanding.

Conflicts of interest

There are no conflicts to declare.

Acknowledgements

References

1   K. Muller, C. Faeh and F. Diederich, *Science*, 2007, **317**, 1881–1886.
2   D. O'Hagan, *Chem. Soc. Rev.*, 2008, **37**, 308–319.
3   S. Purser, P. R. Moore, S. Swallow and V. Gouverneur, *Chem. Soc. Rev.*, 2008, **37**, 320–330.
4   T. Liang, C. N. Neumann and T. Ritter, *Angew. Chem. Int. Ed.*, 2013, **52**, 8214–8264.
5   D. O'Hagan, *J. Fluor. Chem.*, 2010, **131**, 1071–1081.
6   E. A. Ilardi, E. Vitaku and J. T. Njardarson, *J. Med. Chem.*, 2014, **57**, 2832–2842.
7   B. G. de la Torre and F. Albericio, *Molecules*, 2019, **24**, 809.
8   H. Mei, J. Han, S. Fustero, M. Medio-Simon, D. M. Sedgwick, C. Santi, R. Ruzziconi and V. A. Soloshonok, *Chem. – Eur. J.*, 2019, **25**, 11797–11819.
9   J. Fried and E. F. Sabo, *J. Am. Chem. Soc.*, 1954, **76**, 1455–1456.
10 C. Isanbor and D. O'Hagan, *J. Fluor. Chem.*, 2006, **127**, 303–319.
11 "The Top 200 of 2020", ClinCalc DrugStats Database, https://clincalc.com/DrugStats/Top200Drugs.aspx, (accessed February 2020).
12 A. Harsanyi and G. Sandford, *Green Chem.*, 2015, **17**, 2081–2086.
13 S. Caron, *Org. Process Res. Dev.*, 2020, **24**, 470–480.
14 D. O'Hagan and H. Deng, *Chem. Rev.*, 2015, **115**, 634–649.
15 K. B. Kellogg and G. H. Cady, *J. Am. Chem. Soc.*, 1948, **70**, 3986–3990.

16 W. J. Middleton and E. M. Bingham, *J. Am. Chem. Soc.*, 1980, **102**, 4845–4846.
17 M. Schlosser and G. Heinz, *Chem. Ber.*, 1969, **102**, 1944–1953.
18 B. L. Shapiro and M. M. Chrysam, *J. Org. Chem.*, 1973, **38**, 880–893.
19 S. Rozen and O. Lerman, *J. Org. Chem.*, 1980, **45**, 672–678.
20 S. Rozen, O. Lerman, M. Kol and D. Hebel, *J. Org. Chem.*, 1985, **50**, 4753–4758.
21 E. H. Appelman, L. J. Basile and R. C. Thompson, *J. Am. Chem. Soc.*, 1979, **101**, 3384–3385.
22 M. J. Shaw, H. H. Hyman and R. Filler, *J. Am. Chem. Soc.*, 1969, **91**, 1563–1565.
23 B. Zajc and M. Zupan, *J. Chem. Soc. Chem. Commun.*, 1980, 759.
24 R. D. Chambers, M. P. Greenhall and J. Hutchinson, *J. Chem. Soc. Chem. Commun.*, 1995, 21.
25 R. D. Chambers, D. Holling, R. C. H. Spink and G. Sandford, *Lab. Chip*, 2001, **1**, 132.
26 R. D. Chambers, D. Holling, G. Sandford, A. S. Batsanov and J. A. K. Howard, *J. Fluor. Chem.*, 2004, **125**, 661–671.
27 R. D. Chambers, M. A. Fox and G. Sandford, *Lab. Chip*, 2005, **5**, 1132.
28 R. D. Chambers, T. Nakano, M. Parsons, G. Sandford, A. S. Batsanov and J. A. K. Howard, *J. Fluor. Chem.*, 2008, **129**, 811–816.
29 C. B. McPake and G. Sandford, *Org. Process Res. Dev.*, 2012, **16**, 844–851.
30 E. Lisse and G. Sandford, *J. Fluor. Chem.*, 2018, **206**, 117–124.
31 G. S. Lal, G. P. Pez and R. G. Syvret, *Chem. Rev.*, 1996, **96**, 1737–1756.
32 T. Umemoto, K. Kawada and K. Tomita, *Tetrahedron Lett.*, 1986, **27**, 4465–4468.
33 T. Umemoto, K. Harasawa, G. Tomizawa, K. Kawada and K. Tomita, *Bull. Chem. Soc. Jpn.*, 1991, **64**, 1081–1092.
34 A. S. Kiselyov, *Chem. Soc. Rev.*, 2005, **34**, 1031.
35 E. Differding and H. Ofner, *Synlett*, 1991, **1991**, 187–189.
36 R. E. Banks, S. N. Mohialdin-Khaffaf, G. S. Lal, I. Sharif and R. G. Syvret, *J. Chem. Soc. Chem. Commun.*, 1992, 595–596.
37 S. Stavber, M. Zupan, A. J. Poss and G. A. Shia, *Tetrahedron Lett.*, 1995, **36**, 6769–6772.
38 H. Yasui, T. Yamamoto, T. Ishimaru, T. Fukuzumi, E. Tokunaga, K. Akikazu, M. Shiro and N. Shibata, *J. Fluor. Chem.*, 2011, **132**, 222–225.
39 C.-L. Zhu, M. Maeno, F.-G. Zhang, T. Shigehiro, T. Kagawa, K. Kawada, N. Shibata, J.-A. Ma and D. Cahard, *Eur. J. Org. Chem.*, 2013, **2013**, 6501–6505.
40 J. R. Wolstenhulme, J. Rosenqvist, O. Lozano, J. Ilupeju, N. Wurz, K. M. Engle, G. W. Pidgeon, P. R. Moore, G. Sandford and V. Gouverneur, *Angew. Chem. Int. Ed.*, 2013, **52**, 9796–9800.
41 R. Pereira, J. Wolstenhulme, G. Sandford, T. D. W. Claridge, V. Gouverneur and J. Cvengroš, *Chem. Commun.*, 2016, **52**, 1606–1609.
42 D. Meyer, H. Jangra, F. Walther, H. Zipse and P. Renaud, *Nat. Commun.*, 2018, **9**, 4888–4897.
43 J. J. Hart and R. G. Syvret, *J. Fluor. Chem.*, 1999, **100**, 157–161.
44 Manchester University REF Impact Case Study: "The Development of Selectfluor as a Commercial Electrophilic Fluorinating Agent", https://impact.ref.ac.uk/casestudies/CaseStudy.aspx?Id=28087 (accessed February 2020).
45 Y. Zhu, J. Han, J. Wang, N. Shibata, M. Sodeoka, V. A. Soloshonok, J. A. S. Coelho and F. D. Toste, *Chem. Rev.*, 2018, **118**, 3887–3964.
46 Y. Zhou, J. Wang, Z. Gu, S. Wang, W. Zhu, J. L. Aceña, V. A. Soloshonok, K. Izawa and H. Liu, *Chem. Rev.*, 2016, **116**, 422–518.
47 T. A. Miller et al., WO2007/087129, 2007.
48 J. O. Link, J. G. Taylor, L. Xu, M. Mitchell, H. Guo, H. Liu, D. Kato, T. Kirschberg, J. Sun, N. Squires, J. Parrish, T. Keller, Z.-Y. Yang, C. Yang, M. Matles, Y. Wang, K. Wang, G. Cheng, Y. Tian, E. Mogalian, E. Mondou, M. Cornpropst, J. Perry and M. C. Desai, *J. Med. Chem.*, 2014, **57**, 2033–2046.
49 N. R. Curtis, S. H. Davies, M. Gray, S. G. Leach, R. A. McKie, L. E. Vernon and A. J. Walkington, *Org. Process Res. Dev.*, 2015, **19**, 865–871.
50 D. S. Reddy, N. Shibata, J. Nagai, S. Nakamura, T. Toru and S. Kanemasa, *Angew. Chem. Int. Ed.*, 2008, **47**, 164–168.
51 C.-H. Liang, J. Duffield, A. Romero, Y.-H. Chiu, D. Rabuka, S. Yao, S. Sucheck, K. Marby, Y.-K. Shue, Y. Ichikawa, C.-K. Hwang, WO2004080391A2, Optimer Pharmaceuticals, Inc., 2004.
52 D. P. Ip, C. D. Arthur, R. E. Winans and E. H. Appelman, *J. Am. Chem. Soc.*, 1981, **103**, 1964–1968.
53 J. B. Levy and D. M. Sterling, *J. Org. Chem.*, 1985, **50**, 5615–5619.
54 M. Zupan, M. Metelko and S. Stavber, *J. Chem. Soc. Perkin 1*, 1993, 2851.
55 M. Li, X.-S. Xue and J.-P. Cheng, *Acc. Chem. Res.*, 2020, **53**, 182–197.
56 R. E. Banks and G. E. Williamson, *Chem. Ind.*, 1964, 1864–1865.
57 H. Meinert, *Z. Für Chem.*, 1965, **5**, 64.
58 S. T. Purrington and W. A. Jones, *J. Org. Chem.*, 1983, **48**, 761–762.
59 W. E. Barnette, *J. Am. Chem. Soc.*, 1984, **106**, 452–454.
60 R. E. Banks, R. A. Du Boisson and E. Tsiliopoulos, *J. Fluor. Chem.*, 1986, **32**, 461–466.
61 R. E. Banks and I. Sharif, *J. Fluor. Chem.*, 1991, **55**, 207–214.
62 D. D. DesMarteau, U.S. Patent 4,697,011, 1987.
63 E. Differding and R. W. Lang, *Tetrahedron Lett.*, 1988, **29**, 6087–6090.
64 E. Differding and R. W. Lang, *Helv. Chim. Acta*, 1989, **72**, 1248–1252.
65 M. VanderPuy, D. Nalewajek, G. A. Shia, W. J. Wagner, N-Fluoropyridinium Pyridine Heptafluorodiborate, U.S. Patent 4,935,519, 1990.
66 F. A. Davis and W. Han, *Tetrahedron Lett.*, 1991, **32**, 1631–1634.
67 R. Bohlmann, DE 4313664, 1994.
68 I. Cabrera and W. K. Appel, *Tetrahedron*, 1995, **51**, 10205–10208.
69 T. Umemoto and G. Tomizawa, *J. Org. Chem.*, 1995, **60**, 6563–6570.
70 T. Umemoto, M. Nagayoshi, K. Adachi and G. Tomizawa, *J. Org. Chem.*, 1998, **63**, 3379–3385.
71 K. K. Laali, M. Tanaka, F. Forohar, M. Cheng and J. C. Fetzer, *J. Fluor. Chem.*, 1998, **91**, 185–190.
72 Y. Takeuchi, T. Suzuki, A. Satoh, T. Shiragami and N. Shibata, *J. Org. Chem.*, 1999, **64**, 5708–5711.
73 Z. Liu, N. Shibata and Y. Takeuchi, *J. Org. Chem.*, 2000, **65**, 7583–7587.
74 N. Shibata, E. Suzuki and Y. Takeuchi, *J. Am. Chem. Soc.*, 2000, **122**, 10728–10729.
75 D. Cahard, C. Audouard, J.-C. Plaquevent and N. Roques, *Org. Lett.*, 2000, **2**, 3699–3701.
76 H. P. Shunatona, N. Früh, Y.-M. Wang, V. Rauniyar and F. D. Toste, *Angew. Chem. Int. Ed.*, 2013, **52**, 7724–7727.
77 T. Umemoto, S. Fukami, G. Tomizawa, K. Harasawa, K. Kawada and K. Tomita, *J. Am. Chem. Soc.*, 1990, **112**, 8563–8575.

78 T. Umemoto, K. Harasawa, G. Tomizawa, K. Kawada and K. Tomita, *J. Fluor. Chem.*, 1991, **53**, 369–377.

79 A. G. Gilicinski, G. P. Pez, R. G. Syvret and G. S. Lal, *J. Fluor. Chem.*, 1992, **59**, 157–162.

80 P. A. Champagne, J. Desroches, J.-D. Hamel, M. Vandamme and J.-F. Paquin, *Chem. Rev.*, 2015, **115**, 9073–9174.

81 R. E. Banks, M. K. Besheesh, S. N. Mohialdin-Khaffaf and I. Sharif, *J. Chem. Soc. Perkin 1*, 1996, 2069.

82 E. Differding and P. M. Bersier, *Tetrahedron*, 1992, **48**, 1595–1604.

83 E. W. Oliver and D. H. Evans, *J. Electroanal. Chem.*, 1999, **474**, 1–8.

84 Y. Zhang, X.-J. Yang, T. Xie, G.-L. Chen, W.-H. Zhu, X.-Q. Zhang, X.-Y. Yang, X.-Y. Wu, X.-P. He and H.-M. He, *Tetrahedron*, 2013, **69**, 4933–4937.

85 Potentials of Common Reference Electrodes: http://www.consultrsr.net/resources/ref/refpotls.htm (accessed October 2020).

86 C. P. Andrieux, E. Differding, M. Robert and J. M. Saveant, *J. Am. Chem. Soc.*, 1993, **115**, 6592–6599.

87 K. O. Christe and D. A. Dixon, *J. Am. Chem. Soc.*, 1992, **114**, 2978–2985.

88 K. Sudlow and A. A. Woolf, *J. Fluor. Chem.*, 1994, **66**, 9–11.

89 X.-S. Xue, Y. Wang, M. Li and J.-P. Cheng, *J. Org. Chem.*, 2016, **81**, 4280–4289.

90 X. Du, H. Zhang, Y. Yao, Y. Lu, A. Wang, Y. Wang and Z. Li, *Theor. Chem. Acc.*, , DOI:10.1007/s00214-019-2417-2.

91 M. Zupan, J. Iskra and S. Stavber, *J. Org. Chem.*, 1995, **60**, 259–260.

92 P. Toullec, I. Devillers, R. Frantz and A. Togni, *Helv. Chim. Acta*, 2004, **87**, 2706–2711.

93 P. R. Young and W. P. Jencks, *J. Am. Chem. Soc.*, 1977, **99**, 8238–8248.

94 J. P. Richard and W. P. Jencks, *J. Am. Chem. Soc.*, 1982, **104**, 4689–4691.

95 S. Piana, I. Devillers, A. Togni and U. Rothlisberger, *Angew. Chem. Int. Ed.*, 2002, **41**, 979–982.

96 M. Zupan, J. Iskra and S. Stavber, *Tetrahedron*, 1996, **52**, 11341–11348.

97 J. Iskra, M. Zupan and S. Stavber, *Org. Biomol. Chem.*, 2003, **1**, 1528–1531.

98 S. Stavber, T. S. Pečan and M. Zupan, *Tetrahedron*, 2000, **56**, 1929–1936.

99 L. Yang, T. Dong, H. M. Revankar and C.-P. Zhang, *Green Chem.*, 2017, **19**, 3951–3992.

100 M. Zupan, M. Papez and S. Stavber, *J. Fluor. Chem.*, 1996, **78**, 137–140.

101 S. Stavber, T. Sotler Pečan and M. Zupan, *J. Chem. Soc. Perkin Trans. 2*, 2000, 1141–1145.

102 S. Stavber, T. S. Pecan, M. Papez and M. Zupan, *Chem. Commun.*, 1996, 2247.

103 W. L. Orr and N. Kharasch, *J. Am. Chem. Soc.*, 1956, **78**, 1201–1206.

104 M. S. Workentin, N. P. Schepp, L. J. Johnston and D. D. M. Wayner, *J. Am. Chem. Soc.*, 1994, **116**, 1141–1142.

105 J. M. Antelo, J. Crugeiras, J. R. Leis and A. Ríos, *J. Chem. Soc. Perkin Trans. 2*, 2000, 2071–2076.

106 M. Zupan, P. Skulj and S. Stavber, *Tetrahedron*, 2001, **57**, 10027–10031.

107 S. Stavber, M. Jereb and M. Zupan, *J. Phys. Org. Chem.*, 2002, **15**, 56–61.

108 I. Pravst, M. P. Iskra, M. Jereb, M. Zupan and S. Stavber, *Tetrahedron*, 2006, **62**, 4474–4481.

109 G. I. Borodkin, P. A. Zaikin, M. M. Shakirov and V. G. Shubin, *Russ. J. Org. Chem.*, 2007, **43**, 1451–1459.

110 G. I. Borodkin, P. A. Zaikin and V. G. Shubin, *Tetrahedron Lett.*, 2006, **47**, 2639–2642.

111 G. I. Borodkin, I. R. Elanov and V. G. Shubin, *Russ. J. Org. Chem.*, 2015, **51**, 1003–1007.

112 Y. H. Jang, L. C. Sowers, T. Çağin and W. A. Goddard, *J. Phys. Chem. A*, 2001, **105**, 274–280.

113 T. B. Phan, M. Breugst and H. Mayr, *Angew. Chem. Int. Ed.*, 2006, **45**, 3869–3874.

114 For a comprehensive listing of N and E parameters, see https://www.cup.lmu.de/oc/mayr/reaktionsdatenbank/ (Accessed July 2020).

115 D. S. Timofeeva, A. R. Ofial and H. Mayr, *J. Am. Chem. Soc.*, 2018, **140**, 11474–11486.

116 H. Mayr and M. Patz, *Angew. Chem. Int. Ed. Engl.*, 1994, **33**, 938–957.

117 H. Mayr, B. Kempf and A. R. Ofial, *Acc. Chem. Res.*, 2003, **36**, 66–77.

118 X.-H. Duan and H. Mayr, *Org. Lett.*, 2010, **12**, 2238–2241.

119 J. Zhang, J.-D. Yang, H. Zheng, X.-S. Xue, H. Mayr and J.-P. Cheng, *Angew. Chem. Int. Ed.*, 2018, **57**, 12690–12695.

120 N. Rozatian, I. W. Ashworth, G. Sandford and D. R. W. Hodgson, *Chem. Sci.*, 2018, **9**, 8692–8702.

121 N. Rozatian, PhD Thesis, Durham University, 2019.

122 N. Rozatian, A. Beeby, I. W. Ashworth, G. Sandford and D. R. W. Hodgson, *Chem. Sci.*, 2019, **10**, 10318–10330.

123 A. Harsanyi and G. Sandford, *Org. Process Res. Dev.*, 2014, **18**, 981–992.

124 B. Baire, S. Sadhukhan and S. Jampani, *Chem. – Eur. J.*, 2020, **26**, 7145–7175.

125 L. Tang, Z. Yang, J. Jiao, Y. Cui, G. Zou, Q. Zhou, Y. Zhou, W. Rao and X. Ma, *J. Org. Chem.*, 2019, **84**, 10449–10458.

126 S. Wood, S. Etridge, A. Kennedy, J. Percy and D. J. Nelson, *Chem. – Eur. J.*, 2019, **25**, 5574–5585.

127 T. Shono, Y. Matsumura and Y. Nakagawa, *J. Am. Chem. Soc.*, 1974, **96**, 3532–3536.

128 Z. Jin, B. Xu and G. B. Hammond, *Tetrahedron Lett.*, 2011, **52**, 1956–1959.

129 G. I. Borodkin, I. R. Elanov, Y. V. Gatilov and V. G. Shubin, *J. Fluor. Chem.*, 2019, **228**, 109412.

130 N. Rozatian, A. Harsanyi, B. J. Murray, A. S. Hampton, E. J. Chin, A. S. Cook, D. R. W. Hodgson and G. Sandford, *Chem. – Eur. J.*, 2020, **26**, 12027–12035.

131 R. Linnell, *J. Org. Chem.*, 1960, **25**, 290–290.

132 G. Saielli, *Magn. Reson. Chem.*, 2020, **58**, 548–558.

133 I. Kaljurand, A. Kütt, L. Soováli, T. Rodima, V. Mäemets, I. Leito and I. A. Koppel, *J. Org. Chem.*, 2005, **70**, 1019–1028.

134 M. Baidya, S. Kobayashi, F. Brotzel, U. Schmidhammer, E. Riedle and H. Mayr, *Angew. Chem. Int. Ed.*, 2007, **46**, 6176–6179.

135 H. Mayr and A. R. Ofial, *Acc. Chem. Res.*, 2016, **49**, 952–965.

136 K. Sato, G. Sandford, K. Shimizu, S. Akiyama, M. J. Lancashire, D. S. Yufit, A. Tarui, M. Omote, I. Kumadaki, S. Harusawa and A. Ando, *Tetrahedron*, 2016, **72**, 1690–1698.

137 T. Ueno, H. Toda, M. Yasunami and M. Yoshifuji, *Bull. Chem. Soc. Jpn.*, 1996, **69**, 1645–1656.

138 R. S. Muthyala and R. S. H. Liu, *J. Fluor. Chem.*, 1998, **89**, 173–175.

139 F. Sakurai, T. Yukawa and T. Taniguchi, *Org. Lett.*, 2019, **21**, 7254–7257.

140 R. P. Singh and T. Umemoto, in *Encyclopedia of Reagents for Organic Synthesis*, ed. John Wiley & Sons, Ltd, John Wiley & Sons, Ltd, Chichester, UK, 2008.

141 D. D. Steiner, N. Mase and C. F. Barbas, *Angew. Chem. Int. Ed.*, 2005, **44**, 3706–3710.

142 X. Li, X. Shi, X. Li and D. Shi, *Beilstein J. Org. Chem.*, 2019, **15**, 2213–2270.

143 Q. Gu and E. Vessally, *RSC Adv.*, 2020, **10**, 16756–16768.

144 O. Planas, F. Wang, M. Leutzsch and J. Cornella, *Science*, 2020, **367**, 313–317.

145 E. Differding and G. M. Rüegg, *Tetrahedron Lett.*, 1991, **32**, 3815–3818.

146 E. Differding and M. Wehrli, *Tetrahedron Lett.*, 1991, **32**, 3819–3822.

147 S. P. Vincent, M. D. Burkart, C.-Y. Tsai, Z. Zhang and C.-H. Wong, *J. Org. Chem.*, 1999, **64**, 5264–5279.

148 P. T. Nyffeler, S. G. Durón, M. D. Burkart, S. P. Vincent and C.-H. Wong, *Angew. Chem. Int. Ed.*, 2005, **44**, 192–212.

149 J. J. P. Stewart, *J. Comput. Chem.*, 1989, **10**, 209–220.

150 C. Galli and S. D. Giammarino, *J. Chem. Soc. Perkin Trans. 2*, 1994, 1261–1269.

151 K. K. Laali and G. I. Borodkin, *J. Chem. Soc. Perkin Trans. 2*, 2002, 953–957.

152 P. Kralj, M. Zupan and S. Stavber, *J. Org. Chem.*, 2006, **71**, 3880–3888.

153 R. V. Andreev, G. I. Borodkin and V. G. Shubin, *Russ. J. Org. Chem.*, 2009, **45**, 1468–1473.

154 C. Geng, L. Du, F. Liu, R. Zhu and C. Liu, *RSC Adv.*, 2015, **5**, 33385–33391.

155 F. J. Aguilar Troyano, K. Merkens and A. Gómez-Suárez, *Asian J. Org. Chem.*, 2020, **9**, 992–1007.

156 C. R. Pitts, S. Bloom, R. Woltornist, D. J. Auvenshine, L. R. Ryzhkov, M. A. Siegler and T. Lectka, *J. Am. Chem. Soc.*, 2014, **136**, 9780–9791.

157 C. R. Pitts, B. Ling, J. A. Snyder, A. E. Bragg and T. Lectka, *J. Am. Chem. Soc.*, 2016, **138**, 6598–6609.

158 A. Togni, S. L. Rössler, B. J. Jelier, E. Magnier, G. Dagousset and E. M. Carreira, *Angew. Chem. Int. Ed.*, 2020, **59**, 9264–9280.

159 B. Lantaño and A. Postigo, *Org. Biomol. Chem.*, 2017, **15**, 9954–9973.

160 C. Testa, J. Roger, P. Fleurat-Lessard and J.-C. Hierso, *Eur. J. Org. Chem.*, 2019, **2019**, 233–253.

161 S. Qiu, T. Xu, J. Zhou, Y. Guo and G. Liu, *J. Am. Chem. Soc.*, 2010, **132**, 2856–2857.

162 Q. Chen, J. Zeng, X. Yan, Y. Huang, C. Wen, X. Liu and K. Zhang, *J. Org. Chem.*, 2016, **81**, 10043–10048.

163 C.-T. Li, X. Yuan and Z.-Y. Tang, *Tetrahedron Lett.*, 2016, **57**, 5624–5627.

164 Y. Zhang, C. Wen and J. Li, *Org. Biomol. Chem.*, 2018, **16**, 1912–1920.

165 X. Fan, Q. Wang, Y. Wei and M. Shi, *Chem. Commun.*, 2018, **54**, 10503–10506.

166 J. Zhou, Y. Fang, F. Wang and J. Li, *Org. Biomol. Chem.*, 2019, **17**, 4470–4474.

167 R. Jójárt, P. Traj, É. Kovács, Á. Horváth, G. Schneider, M. Szécsi, A. Pál, G. Paragi and E. Mernyák, *Molecules*, 2019, **24**, 1783.

168 G. Bucher and J. C. Scaiano, *J. Am. Chem. Soc.*, 1994, **116**, 10076–10079.

169 C. P. Johnston, T. H. West, R. E. Dooley, M. Reid, A. B. Jones, E. J. King, A. G. Leach and G. C. Lloyd-Jones, *J. Am. Chem. Soc.*, 2018, **140**, 11112–11124.

170 A. García-Domínguez, T. H. West, J. J. Primozic, K. M. Grant, C. P. Johnston, G. G. Cumming, A. G. Leach and G. C. Lloyd-Jones, *J. Am. Chem. Soc.*, 2020, **142**, 14649–14663.

171 T. Scattolin, K. Deckers and F. Schoenebeck, *Org. Lett.*, 2017, **19**, 5740–5743.

172 T. Scattolin, S. Bouayad-Gervais and F. Schoenebeck, *Nature*, 2019, **573**, 102–107.

173 A. Turksoy, T. Scattolin, S. Bouayad-Gervais and F. Schoenebeck, *Chem. – Eur. J.*, 2020, **26**, 2183–2186.

174 G. Roagna, D. M. H. Ascough, F. Ibba, A. C. Vicini, A. Fontana, K. E. Christensen, A. Peschiulli, D. Oehlrich, A. Misale, A. A. Trabanco, R. S. Paton, G. Pupo and V. Gouverneur, *J. Am. Chem. Soc.*, 2020, **142**, 14045–14051.

TOC entry text:

A comprehensive review of past and present approaches towards qualitative and quantitative rankings of the reactivities of electrophilic fluorinating agents.